Pergamon

Geochimica et Cosmochimica Acta, Vol. 62, No. 12, pp. 2179–2196, 1998

0016-7037/98 $19.00 + .00

PII S0016-7037(98)00137-9

Petrology and geochemistry of target rocks from the Bosumtwi impact structure, Ghana, and comparison with Ivory Coast tektites

CHRISTIAN KOEBERL,[1,*] WOLF UWE REIMOLD,[2] JOEL D. BLUM,[3] and C. PAGE CHAMBERLAIN[3]

[1]Institute of Geochemistry, University of Vienna, Althanstrasse 14, A-1090 Vienna, Austria
[2]Department of Geology, University of the Witwatersrand, P.O. Wits, Johannesburg 2050, South Africa
[3]Department of Earth Sciences, Dartmouth College, Hanover, New Hampshire 03755, USA

(*Received October* 24, 1997; *accepted in revised form March* 19, 1998)

Abstract—The 10.5 km diameter Bosumtwi crater in Ghana, West Africa, is the most likely source crater for the Ivory Coast tektites, as the tektites and the crater have the same age (1.07 Ma), and there are close similarities between the isotopic and chemical compositions of the tektites and crater rocks. The crater is excavated in 2.1–2.2 Ga old metasediments and metavolcanics of the Birimian Supergroup. Here we present the first integrated petrographic and geochemical study of rocks from the Bosumtwi impact crater. A variety of target rocks from the Bosumtwi impact structure were selected to represent the major rock types that have been described before, resulting in four groups: shale, phyllite-graywacke, and two different types of granites (from dispersed dikes and from the so-called Pepiakese intrusion at the northeastern side of the crater). These rocks were analyzed for their major and trace element composition and their petrographic characteristics. In addition, representative samples were also analyzed for their O, Sr, and Nd isotopic compositions. The target rocks do not show any unambiguous evidence of shock metamorphism (i.e., planar deformation features, PDFs). Distinct impact-characteristic shock effects (PDFs) were identified only in clasts within suevite-derived melt fragments. The compositional range of the target rocks is significantly wider than that of the Ivory Coast tektites, but overlap the tektite compositions. A best-fit line for the Bosumtwi crater rocks in a Rb-Sr isotope evolution diagram yields an "age" of 1.98 Ga, and an initial $^{87}Sr/^{86}Sr$ ratio of 0.701, which is close to results previously obtained for granitoid intrusions in the Birimian of Ghana. Our Nd isotopic data yield depleted mantle model ages ranging from 2.16 to 2.64 Ga, and ϵ_{Nd} values of −17.2 to −25.9‰. Harmonic least-squares (HMX) mixing calculations were able to reproduce the composition of Ivory Coast tektites from a mixture of Bosumtwi country rocks that include about 70% phyllite-graywacke, 16% granite dike, and 14% Pepiakese granite. The oxygen isotopic composition of the metasedimentary rocks and granite dikes ($\delta^{18}O = 11.3$–13.6‰) and the tektites ($\delta^{18}O = 11.7$–12.9‰, also this work) agree fairly well, while the Pepiakese granites have lower values ($\delta^{18}O = 8.6$–9.0‰), indicating that only minor amounts of these rocks were incorporated in the formation of the Ivory Coast tektites. The large variation in Sr and Nd isotopic compositions of the target rocks do not allow the unambiguous identification of distinct endmember compositions, but in both a $^{87}Sr/^{86}Sr$ vs. 1/Sr plot and an ϵ_{Sr} vs. ϵ_{Nd} diagram, the tektites plot within the area occupied by the metasedimentary and granitic Bosumtwi crater rocks. Thus, our data support the interpretation that the composition of the Ivory Coast tektites is similar to that of rocks exposed at the Bosumtwi impact structure, indicating formation during the same impact event.

1. INTRODUCTION

The Bosumtwi impact crater is located about 30 km southeast of the town of Kumasi in the Ashanti Province, Ghana (West Africa), centered at 06°32′N and 01°25′W (Fig. 1). The crater is almost completely filled by Lake Bosumtwi (e.g., Turner et al., 1996) and has a rim-to-rim diameter of about 10.5 km. The lake has a diameter of about 8 km and a current maximum depth of about 80 m. The crater rim rises about 250–300 m above the lake level. On topographic maps a subtle concentric outer ridge (with a total diameter of about 18 km) appears in some sections of the structure, but its origin is still not clear (cf. Jones et al., 1981; Reimold et al., 1998). The crater has an age of 1.07 Ma (cf. Storzer and Wagner, 1977; Koeberl et al., 1997a) and was excavated in lower greenschist facies metasediments of the 2.1–2.2 Ga Birimian Supergroup (cf. Wright et al., 1985; Leube et al., 1990).

*Author to whom correspondence should be addressed (christian.koeberl@univie.ac.at).

The Birimian Supergroup has commonly been subdivided into the Lower Birimian, dominated by metasediments, and the Upper Birimian, dominated by greenstone-type metavolcanics (e.g., Junner, 1937). These altered metavolcanics are present to the west and southwest of the Bosumtwi crater (Fig. 2). Further to the west and southwest are Tarkwaian sediments, which are clastic sediments formed by erosion of Birimian rocks. The Birimian Supergroup in Ghana is present in the form of five parallel, evenly spaced, volcanic belts several hundred kilometers in length, which are separated by basins containing dacitic volcaniclastics, wackes, argillitic sediments, and granitoids (e.g., Wright et al., 1985; Leube et al., 1990). New geochronologic data indicate that there is no evidence for a separation of Lower and Upper Birimian in time, with rocks from both groups having a Sm-Nd isochron age of 2.17 ± 0.07 Ga (cf. Leube et al., 1990; Taylor et al., 1992; Davis et al., 1994; Hirdes et al., 1996). These authors argued that both lavas and sedimentary rocks were deposited contemporaneously. A variety of granitoids intruded synorogenically (the sedimentary-basin granitoids of the Cape Coast type) or late-orogenically

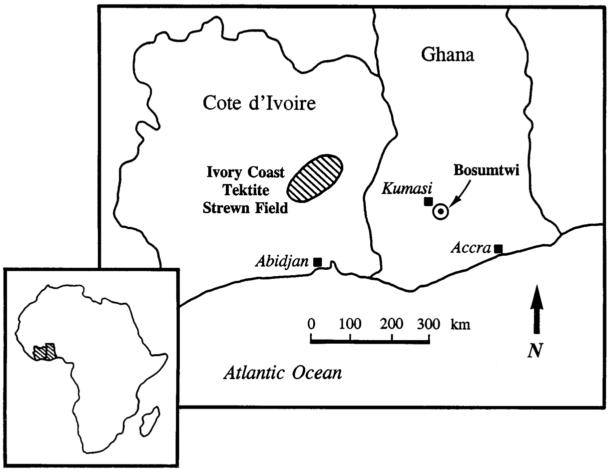

Fig. 1. Geographical location of the Bosumtwi impact crater, Ghana, in relation to the Ivory Coast tektite strewn field.

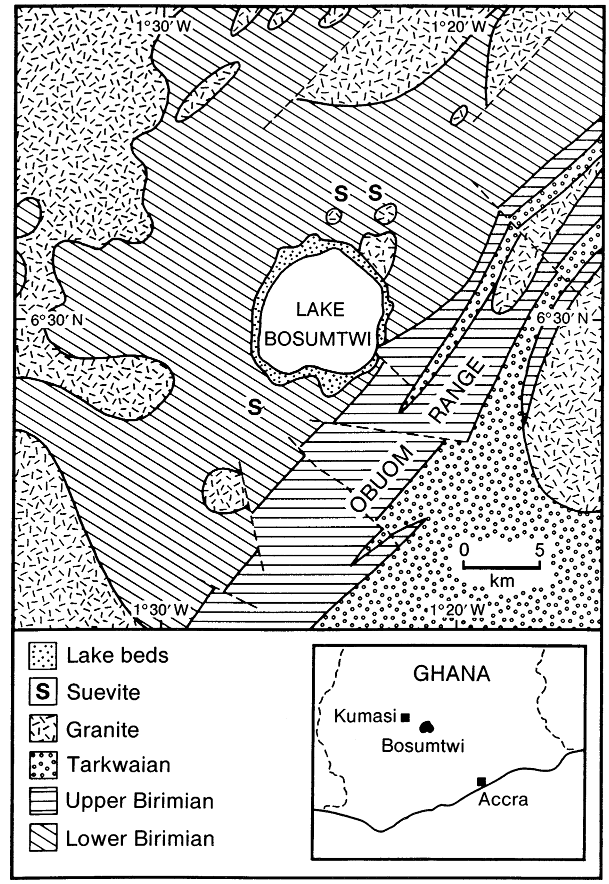

Fig. 2. Schematic geological map of the Bosumtwi impact structure and surroundings, after Jones et al. (1981). The distinction between Upper and Lower Birimian has recently been questioned on the basis of new dating (cf. Leube et al., 1990; Hirdes et al., 1996) and may only represent a difference in rock type variation (i.e., preponderance of metamorphosed volcanic rocks vs. metasediments in the Upper and Lower Birimian, respectively), but not in age.

(the volcanic-belt granitoids of the Dixcove type) with the folding of the basins following the termination of the volcanic activity (Leube et al., 1990).

In general, the regional geology around the Bosumtwi crater (Fig. 2) is dominated by graywackes and sandstone/quartzitic rocks, but especially in the northeastern and southern sectors shale and minor mica schist are also present (Woodfield, 1966; Moon and Mason, 1967; field observations by W. U. Reimold and C. Koeberl in 1997). Several Proterozoic granitic intrusions occur in the region around the crater, and a small number of strongly weathered granitic dikes were observed in the crater rim as well (Jones, 1985a; Reimold et al., 1997, 1998). The granitic component of the target region is estimated at <2% (Reimold et al., 1997). The most detailed geological survey of the crater area was reported by Junner (1937), and is the basis of the schematic geological map of Jones et al. (1981), and of Fig. 2, but should be reinterpreted based on the recent geochronologic work mentioned above.

Lake Bosumtwi has been known to the scientific community since late last century, but its origin was the subject of a controversy, as described by Junner (1937) and Jones (1985b): Fergusson (1902) thought it was not of volcanic origin, Kitson (1916) interpreted it as a subsidence feature, Maclaren (1931) thought the crater was of impact origin, Rohleder (1936) preferred an explosive (endogenic) explanation. In the early 1960s, renewed interest led to additional studies and continuing controversy, caused partly by an incomplete (at that time) understanding of impact processes (Bampo, 1963; Smit, 1964). Subsequently, outcrops of suevitic breccia, similar to that found at the Ries impact structure in Germany, were found around the crater (e.g., Chao, 1968; Jones et al., 1981), and the high-pressure quartz modification coesite (Littler et al., 1961), as well as Ni-rich iron spherules and baddeleyite, the high-temperature decomposition product of zircon, were discovered in vesicular glass from the crater rim (El Goresy, 1966; El Goresy et al., 1968). All these lines of evidence support an impact origin for the structure.

The Bosumtwi crater is of special interest as the likely source crater for the Ivory Coast tektites, which were first reported in 1934 (Lacroix, 1934) from a small area of about 40 km radius within the Ivory Coast (Cote d'Ivoire), West Africa (Fig. 1). Later, more samples were recovered by, e.g., Gentner (1966) and Saul (1969). Microtektites were found in deep-sea cores off the coast of Western Africa (Glass, 1968, 1969) and have been related to the tektites found on land. The geographical distribution of microtektite-bearing deep-sea cores is used to determine the extent of the strewn field (Glass and Zwart, 1979; Glass et al., 1979, 1991). As tektites are formed during hypervelocity impacts on Earth and represent melts of surfical, predominantly sedimentary, precursor rocks of upper crustal composition (see Koeberl, 1994, for a recent review), a suitable source crater needs to be identified.

A variety of arguments was used to conclude that Bosumtwi is most likely this source crater, including similar chemical compositions (Schnetzler et al., 1967; Jones, 1985a) and similar isotopic characteristics for the tektites and rocks found at the crater (e.g., Schnetzler et al., 1966; Lippolt and Wasserburg, 1966; Shaw and Wasserburg, 1982), and the similar ages of tektites and Bosumtwi impact glasses (e.g., Gentner et al.,

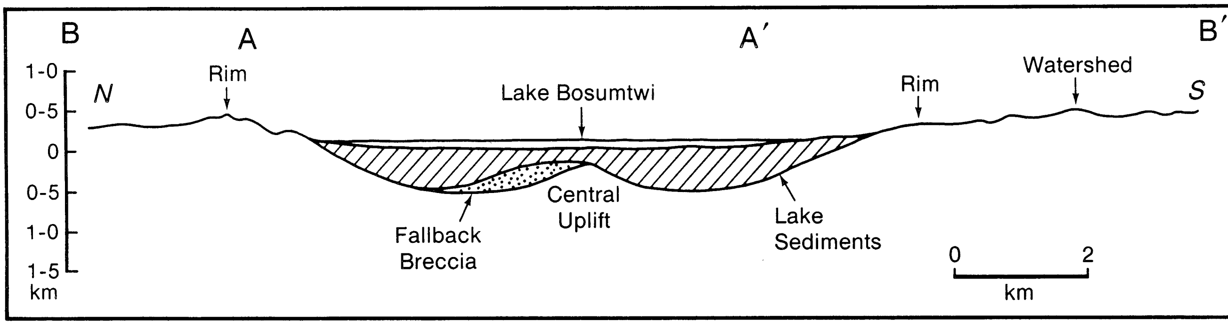

Fig. 3. Hypothetical north-south cross section of the Bosumtwi impact structure, after Jones et al. (1981). At the present time, no information is available regarding the existence (or position) of a central uplift or fallback (or any other) breccia below the lake sediments (which are of unknown thickness).

1964, 1967; Storzer and Wagner 1977). While these early published ages range from 0.71 to 1.2 Ma for Ivory Coast tektites, recent precise fission track and step-heating ^{40}Ar-^{39}Ar dating on both Ivory Coast tektites and Bosumtwi impact glass established a reliable age of 1.07 $\pm$ 0.05 Ma for the Bosumtwi impact event (Koeberl et al., 1997a).

Our knowledge of the Bosumtwi impact structure is still fairly limited. No detailed petrographical analyses of the crater rocks are available, and no integrated petrographical and geochemical studies have been done. The structural aspects of the crater are unknown, and while some general geophysical studies of the area are available (Jones et al., 1981), no detailed geophysical measurements of the crater itself have been published. Understanding the subsurface crater structure is important for determining the connection between the various crater rocks, breccias, and melts, providing constraints for further geophysical studies, and for establishing the presence of a proposed subsurface gas pool under the crater (Jones, 1983), but so far only a hypothetical cross-section (see Fig. 3, after Jones et al., 1981), based on analogy with other impact structures, can be inferred.

Recently, additional field work was conducted at the Bosumtwi impact crater, e.g., to study the structural aspects of the crater rim (Koeberl et al., 1997b; Reimold et al., 1997). In addition, a high-resolution aerogeophysical survey across the structure was conducted in early 1997, to obtain more detailed information of the subsurface structure below and beyond the lake (cf. Koeberl et al., 1997b); the results of these and related studies will be reported elsewhere. In the present paper, we report on petrographic studies, major and trace element compositions, and oxygen, Sr, and Nd isotope data of a set of rocks from the Bosumtwi impact crater, and present comparisons with data for Ivory Coast tektites.

2. SAMPLES AND EXPERIMENTAL METHODS

2.1. Samples

Centimeter to decimeter sized cuts of seventeen of the target rocks from the Bosumtwi crater that were previously analyzed for major and selected minor elements by Jones (1985a) were obtained for this study through the courtesy of Dr. W. B. Jones (Wrexham, UK). The same set of samples, which have the prefix "J" was used in the Re-Os isotope study of Koeberl and Shirey (1993). In addition, six samples of granite and suevitic impact breccia (prefix: B) were obtained from the collection of the Smithsonian Institution, Washington, DC, USA. Petrographic thin sections for optical microscopy were cut from each of the samples. Parts of most of the remaining mass of the samples were then prepared for major and trace element analysis and isotope analysis. Samples were crushed in polyethylene wrappers. Subsequently, the rock chips were powdered with agate or boron carbide mills, to avoid any contamination.

2.2. Chemical Analyses

Major element analyses were done on powdered samples by standard X-ray fluorescence (XRF) procedures (see Reimold et al., 1994, for details on procedures, precision, and accuracy). The concentrations of V, Cu, Y, and Nb were also determined by XRF analysis. All other trace elements were determined on 200-mg-aliquots by instrumental neutron activation analysis (INAA), following procedures described by Koeberl et al. (1987) and Koeberl (1993). For most samples, Sr and Zr concentrations were determined by both XRF and INAA, and for some of the low abundance samples, Ni data were also obtained by XRF.

2.3. Isotope Analyses

Aliquots of the same powders used for major and trace element chemical analysis were used for isotopic analysis. Fifty mg was used for each oxygen isotope analysis and 100 mg was used for Sr and Nd isotope analyses. Oxygen was extracted from these silicate samples and converted to CO_2 following the conventional BrF_5 method (Clayton and Mayeda, 1963). The extracted CO_2 was analyzed for O isotopic composition on a dual-inlet Finnigan Delta E mass spectrometer. Analyses are reported relative to standard mean ocean water (SMOW). Measurements of NBS-18 and NBS-28 yielded $\delta^{18}O$ values of 7.2 $\pm$ 0.2‰ and 9.6 $\pm$ 0.2‰, respectively.

For analysis of Sr and Nd isotopes rock powders were digested with a mixture of HF and $HClO_4$, and separated into Sr, and total rare earth element (REE) fractions using a 1 $\times$ 17 cm quartz cation exchange column loaded with 200–400 mesh Bio-Rad AG 50W-X8 resin using HCl as the eluent. Separation of Nd from the REE fraction was accomplished using a 0.2 $\times$ 33 cm quartz cation exchange column loaded with $-$400 mesh Bio-Rad AG 50W-X4 resin using 2-methyllactic acid as the eluent. Approximately 100 ng samples of Sr were loaded onto W filaments with Ta_2O_5 powder and $\sim$100 ng samples of Nd were loaded onto Re filaments with dilute HCl. Isotope ratios were measured on a multiple-collector Finnigan MAT 262 thermal ionization mass spectrometer with Sr and Nd isotope ratios normalized to $^{86}Sr/^{88}Sr = 0.1194$ and $^{146}Nd/^{144}Nd = 0.7219$, respectively. Reported uncertainties in isotope ratios are 2σ of the mean of 100–200 ratios for Nd and Sr. Possible isobaric interferences on ^{87}Sr by ^{87}Rb and ^{144}Nd by ^{144}Sm were monitored using ^{85}Rb and ^{147}Sm and small corrections (less than 2 parts in 10^5 of the measured $^{87}Sr/^{86}Sr$ and $^{143}Nd/^{144}Nd$ ratios) were made for isobaric interference. Analyses of NBS-987 and Caltech nNdβ during the time of this investigation yielded $^{87}Sr/^{86}Sr$ =

0.710243 ± 22 (2σ, n = 44) and ^{143}Nd/^{144}Nd = 0.511899 ± 16 (2σ, n = 30), respectively. Total procedural blanks were <20 pg Nd and <70 pg Sr and are negligible. The ^{87}Rb and ^{147}Sm decay constants used in calculations are those recommended in Blum (1995).

3. RESULTS AND DISCUSSION

3.1. Petrography

Previous workers have concentrated on the elemental and isotopic compositions of Bosumtwi crater rocks. So far, little information has been available on their petrography (Chao, 1968). Jones (1985) attempted to collect a representative suite of rocks from the Bosumtwi crater for chemical analyses, but did not report on any petrographic studies of these rocks. To gain a better understanding about the rock types present at the crater, and their shock metamorphic stage, we obtained petrographic thin sections of the rocks that were previously studied by Jones (1985a), and also performed more extensive chemical and isotopic analyses on these samples.

As mentioned before, the country rocks in the region of the Bosumtwi crater consist mainly of Birimian metasediments of early Proterozoic age. These rocks are characterized by a consistent NE-SW foliation trend (e.g., Junner, 1937). Their local appearance in the field is either relatively massive to very well laminated (Reimold et al., 1998). Compositionally these rocks can be classified as arkoses, greywackes, sandstones, shales, and schists. It appears likely that some fine-grained mica schists have, in the past, been referred to as phyllite. These metasediments are locally intruded by granitic complexes and dikes, probably mainly belonging to the Kumasi-type granitoid intrusions, for which an age of 2.0–2.1 Ga has been obtained (e.g., Taylor et al., 1992; Hirdes et al., 1992). In addition, quartz veining is quite abundant. Locally, suevite has been reported, especially to the north and south of the crater.

The sample suite available for this study is representative of this range of lithologies (cf. Jones, 1985a). Short petrographic descriptions of the rocks are summarized in Table 1 and photomicrographs of some of the samples are shown in Fig. 5. Of the samples originally analyzed by Jones (1985a), some were reclassified based on the petrographic findings. The distinction between graywacke and phyllite is not well established, and several transitionary specimens were encountered. Furthermore, we classified some samples as shales that were previously classified as phyllites. All metasedimentary rocks display a strong fabric (Fig. 5a,b). However, in addition to the schistosity displayed by all samples from this region, several samples have been deformed and exhibit mylonitic shear textures (S-C fabrics). Most metasediment samples do not display any late deformation, with the exception of sample J494, which must have been deformed in a ductile manner after the initial mylonitization event. None of the metasediment samples displays any evidence of characteristic shock effects.

A number of granite samples were studied as well, all of which are completely devoid of shock deformation. These granites were obtained from two different settings. First, samples J493 and J505 are from small dikes of granitoids that are present around the crater (Fig. 4; also, cf. Koeberl et al., 1997b). These samples have been described by Jones (1985a) as microgranites, which is, however, not an appropriate term; thus, for the purposes of this paper we call them "granite dikes." The samples of this type studied here are relatively unaltered (Fig. 5c,d). In contrast, samples J507-509 are from a larger intrusive granitoid body on the northeastern side of the lake and have been termed "Pepiakese granites" after the location of the intrusion. It is not clear if they represent the same intrusive event as the small dikes mentioned above. Both granitoid types could be related to the Kumasi-type granite described by, e.g., Taylor et al. (1992). Sample J507 displays a significant degree of intragranular, irregular microfracturing. Samples of this group vary somewhat with regard to their degrees of alteration (sample J508 being rather strongly weathered). In addition, a single sample of granodiorite was analyzed (sample J509), which contains more mafic minerals (biotite, amphibole) than the other granitoid specimens.

The remaining samples, from the Smithsonian Institute collection, are small melt fragments that were originally part of suevite samples. Sample B026, B034, and B075 represent glassy, vesicular melt rock, which is, in patches, devitrified. B075 is unique in that it constitutes a frothy melt (Fig. 6a), which seems to be composed of tiny glass spherules. It also does not contain many clasts. In contrast, the other two melt samples contain many inclusions, among which a number of shocked quartz clasts with one set or multiple sets of planar deformation features (PDFs, see below) could be recognized (Fig. 6b,c). lt appears that many of the clasts in these melt rocks are granitoid derived. In sample B034, a few orthoclase crystals displaying mechanical twinning were observed.

Finally, sample B091 is a granitic breccia characterized by large annealed areas. Alteration is strong and secondary carbonate is abundant. In several small patches a devitrified, silica-rich melt occurs, similar to patches in dikes recently sampled in the crater wall of the Bosumtwi crater. However, these partially melted samples are all based on metasedimentary precursor material (cf. Koeberl et al., 1997b; Reimold et al., 1997). No shock metamorphic effects were noted in this sample, which nonetheless must be considered a monomict lithic impact breccia.

Shock metamorphic effects in rocks from the Bosumtwi crater were first mentioned by Littler et al. (1961) and Chao (1968), who described the presence of coesite and shocked minerals in suevite (ejecta) from outside the crater rim. Our study confirms the presence of PDFs in quartz within clasts in suevites. PDFs in quartz, which form in nature only during hypervelocity impact (see, e.g., Grieve et al., 1996, and references therein), are parallel submicroscopic to microscopic zones consisting of amorphous silica with a thickness of about <1–3 μm that are spaced about 2–10 μm apart, which occur in planes corresponding to specific crystallographic orientations. We did not find a large enough number of shocked quartz grains in our present sample suite to perform a statistically relevant universal stage study of the crystallographic orientations of the PDFs. It is interesting that none of the country rocks—some of which were exposed directly at the crater rim—show any evidence of shock metamorphism. Shocked minerals are restricted to clasts within suevitic breccias, which occur outside of the crater rim (but inside the outer ridge zone) and which represent ejecta from the lower part of the crater.

Table 1. Petrographic Observations on Bosumtwi Impact Crater Rocks.

Sample	Description
Shale	
J490	Mylonitized shale, unshocked
J497	Mylonitic shale; strong crenulation cleavage, very nice S-C fabric; unshocked
J502	Shale - interbedded with somewhat coarser-grained and quartz-richer, but still pelitic bands; mylonitized; cut by several quartz veins; unshocked
J503	Shale with chert lenses; unshocked
Phyllite-Graywacke	
J491	Fine-grained, mylonitic rock, transitional between phyllite and graywacke sample; i.e., contains more biotite than J501; unshocked
J492	Weakly ductile-deformed rock, transitional between graywacke and phyllite, containing abundant mica, but also considerable amounts of large quartz and feldspar grains; unshocked
J494	Mylonitic graywacke; evidence for second-stage, postmylonitization shear deformation; unshocked
J495	Mylonitic graywacke-phyllite (the transitional variety); unshocked
J496	Mylonitic graywacke; unshocked
J501	Mylonitic graywacke; unshocked
J504	Mylonitic graywacke; unshocked
J506	Graywacke, not mylonitized; unshocked
B096	Mylonitic phyllite, with abundant sericite; unshocked
Granite Dike	
J493	Fine-grained granite; unshocked
J505	Medium-grained granite with strongly altered (sericitized) plagioclase; unshocked
B001	Fresh, undeformed biotite-granite; unshocked
Pepiakese Rocks ("Pepiakese Granite")	
J507	Medium-grained granite; predominantly composed of plagioclase, with the rest being alkali feldspar, quartz, some sericite (secondary), and muscovite (maybe primary); no characteristic shock effects, but abundant intragranular, irregular fracturing
J508	Large amphibole crystals in a plagioclase-rich mass, which is strongly chloritized and sericitized; plagioclase is strongly altered to patches of relatively coarse-grained sericite; may have been an amphibole-biotite-diorite before alteration; unshocked
J509	Biotite-rich (30 vol%) granite; medium-grained; unshocked
Suevite	
B026	Glassy, vesicular melt rock, in patches devitrified; contains 2 quartz grains with 1 set of PDFs each
B034	Glassy, vesicular impact melt, similar to B026; 1 orthoclase clast with multiple sets of PDFs, 1 quartz crystal with 2 sets of PDFs; clasts are granite-derived; somewhat clast-richer than B026; noticeable alteration effects; some orthoclase grains display mechanical twinning
B075	Highly vesicular melt rock resembling "froth" made up of tiny isotropic globules
B091	Granitic breccia, after biotite-granite, with large annealed areas; strong alteration (carbonates); contains patches of totally devitrified silica-rich melt; no obvious shock effects in mineral and rock fragments

Samples with a J prefix are from Jones (1985a). Samples with a B prefix are from the Smithsonian Institution (sample number references: B001 = 116517.0001/BCC-1-64; B026 = 116517.0026/BCC-5A-64; B034 = 116517.0034/BCC-5A-64-10; B075 = 116517.0075/BCC-8B-64; B091 = 116517.0091/BCC-9-64-3; B096 = 116517.0096/BCC-10-64).

3.2. Chemical Composition of Bosumtwi Crater Rocks

The results of our major and trace element analyses on Bosumtwi crater rocks are reported in Table 2a, while averages and ranges, and a comparison with Ivory Coast tektite values, are given in Table 2b. In general, the target rocks cover a wide range in chemical composition, both for major and trace element abundances. Based on petrographical and chemical data, we have subdivided the target rocks into four groups: shale, phyllite-graywacke, granite dikes, and Pepiakese granite. The results are mostly in good agreement with Jones (1985a) for the major elements, but some of the trace element data, especially the rare earth elements (REE), show some discrepancies, probably due to the lower precision of the earlier data and/or sample heterogeneity.

The shales have a low silica content (average about 55.6

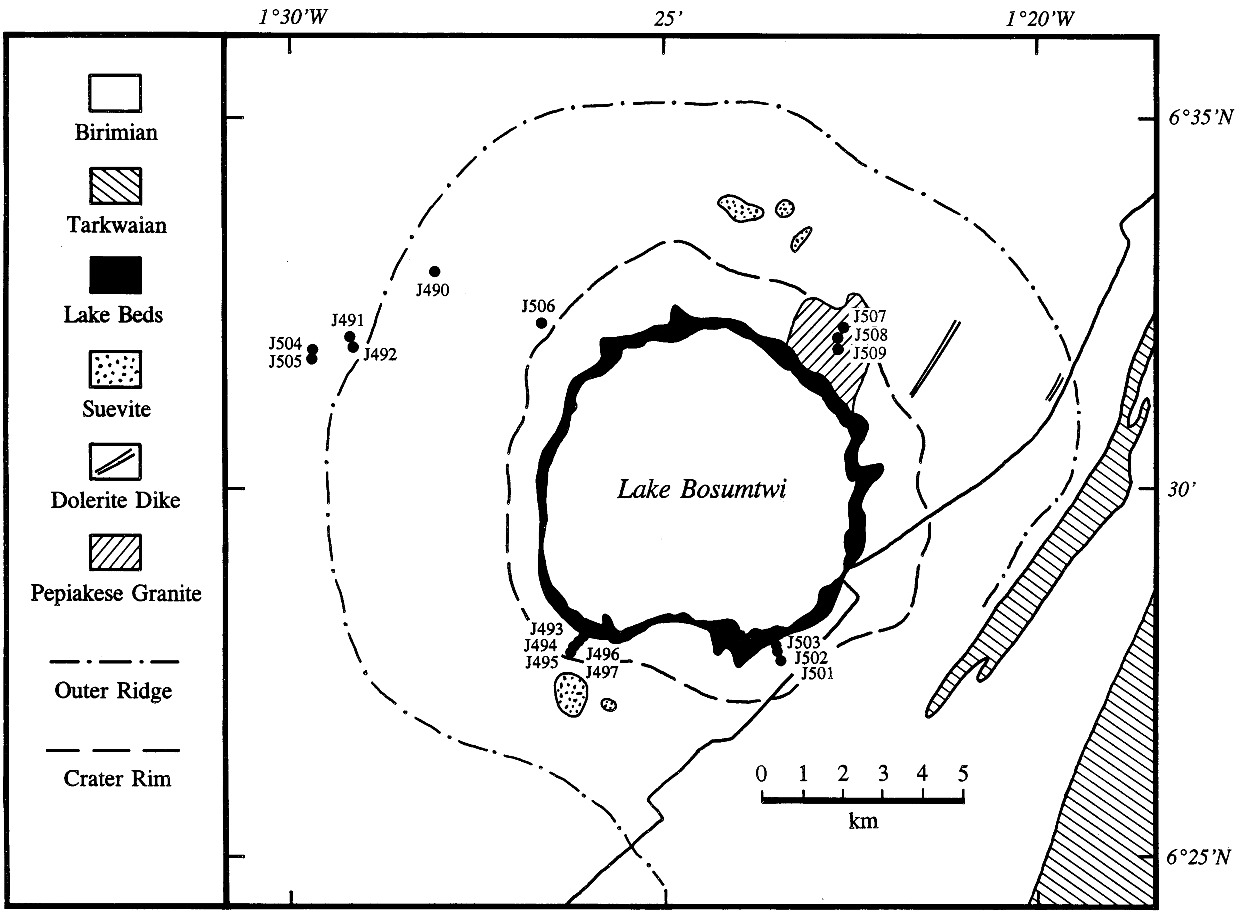

Fig. 4. Location of samples analyzed in the present study, after Jones (1985a). Sample positions are indicated by small solid circles. Also shown are the outline of the crater rim (dashed line) and a possible outer ridge (dot-dashed line), which is evident in the form of a series of slight topographic elevations around about three fourth of the crater. The solid line from bottom center to upper right of the map indicates the area where altered volcanic rocks are more important (to the right) and metasedimentary rocks (to the left) account for most of the country rock.

wt%) and a fairly limited range in composition. In agreement with the petrological observations, the group of graywackes and phyllites is somewhat more variable in composition, but clearly distinct from the shales. Relatively high contents of chalcophile elements, such as V, Cu, Zn, and As, are noticeable in most samples and may have been derived from mineralized zones associated with the nearby Tarkwaian sediments. This is also supported by the consistently high Au contents of the Bosumtwi samples.

The compositions of the two granites collected from granite dikes are fairly similar and are somewhat similar to the compositions of sedimentary-basin granitoids of the Cape Coast type reported by Leube et al. (1990), but the Bosumtwi granite dikes have lower Ca and higher Fe and Mg contents than the average of those rocks. The one granite sample from the Smithsonian collection (B001) was too small to obtain a representative major element composition. The sample used for trace element analysis was quartz-rich and, therefore, not easily comparable to the other granite samples (which were obtained from a more representative amount of rock). In contrast to the granite dikes, the granitoids from the Pepiakese intrusion (samples J507-9) have highly variable compositions and appear to be strongly altered. Sample J507 has a high Na content, which can partially be attributed to the presence of abundant plagioclase, which is the main phase observed in thin section. Some exchange of K for Na as a result of alteration may also have been involved. Samples J508 and J509 are characterized by very high Fe, Mg, and Ca contents, probably due to extensive chloritization and a significant proportion of amphibole and/or biotite in these samples.

Figure 7 shows the average target rock compositions (Table 2b) in a chondrite-normalized REE diagram. The shale, graywacke, and phyllite samples show very similar patterns, in agreement with their mineralogy. Both have slight negative Eu anomalies and negative Ce anomalies, indicating alteration by weathering. The shales have slightly higher heavy REE contents and a more pronounced Eu anomaly than the graywacke samples. The other phyllite-graywacke samples, as well as the two types of granite, do not show a negative Ce anomaly. The steep REE patterns of the granitoids, without a negative Eu anomaly, are typical of Archean crustal rocks (cf. Taylor and McLennan, 1985).

(a) (b) (c) (d) (e) (f)

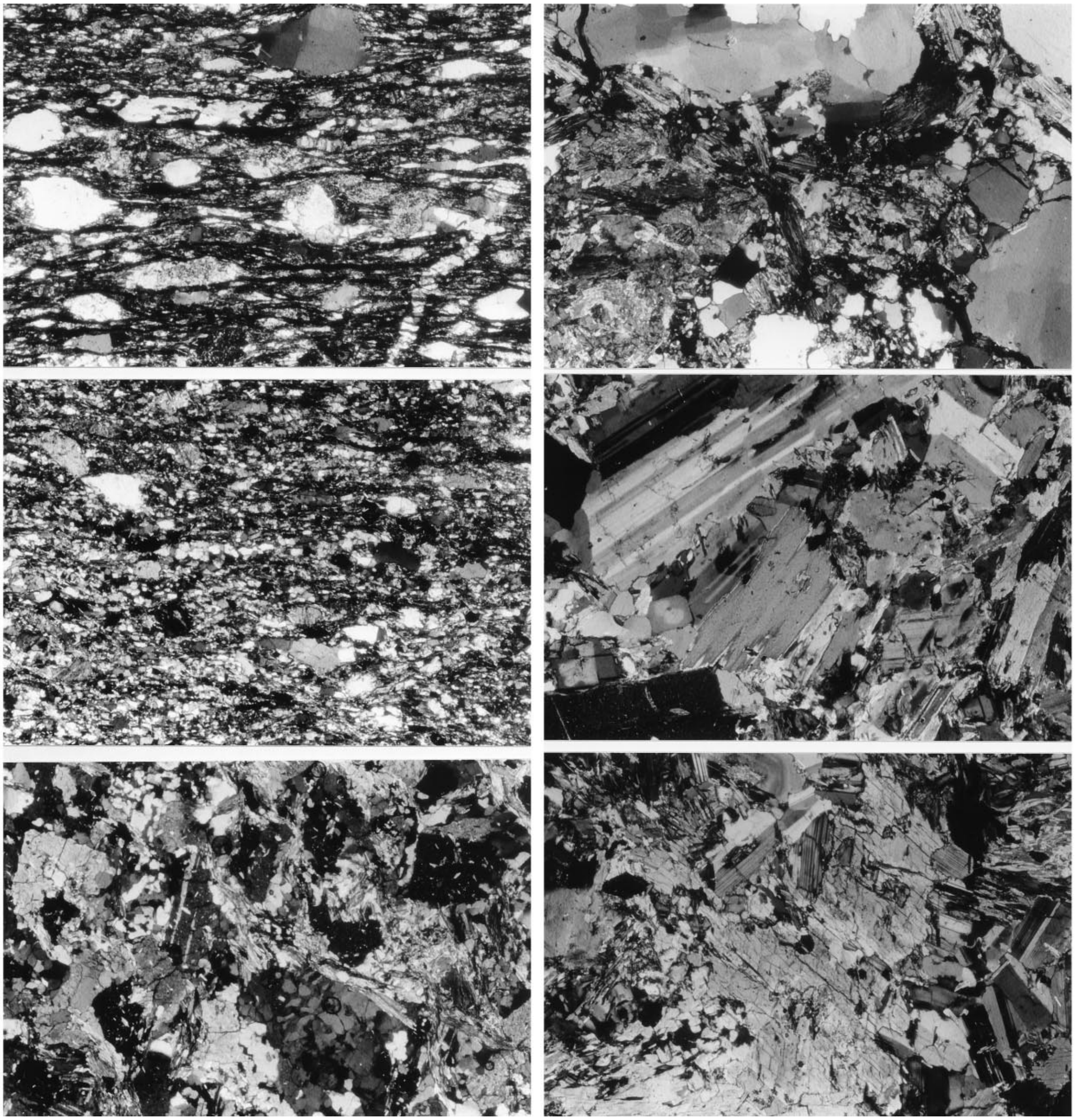

Fig. 5. Photomicrographs of thin sections of representative rocks from the Bosumtwi impact structure. All photos are taken in transmitted light with crossed polarizers. Each image is 3.5 mm wide. (a) Mylonitic graywacke with strongly extended quartz porphyroblasts, sample J501. (b) Mylonitic graywacke with strongly extended quartz ribbons, sample J495. (c) Fine-grained granite with minor micropegmatitic component, sample J493. (d) Biotite-granite, showing minor brecciation and slight annealing, sample J505. (e) Biotite-rich granite (from the Pepiakese location), with large plagioclase grains, sample J509. (f) Altered and somewhat brecciated amphibole and plagioclase-rich Pepiakese granitoid, sample J508.

The small size of the suevite-derived glassy melt fragments, and the general heterogeneity of the samples, did not yield enough material for major element analyses. The trace element analyses (Table 2a), which were performed on small (100 mg sized) chips of mainly glassy material, show some variations in the compositions of the three glassy samples (B026, B034, B075) and the devitrified melt/breccia sample (B091). The part of sample B075 that was used for trace element measurement is a quartz-rich glass fragment, as is evident from the low overall elemental contents. The other three samples have compositions that are similar to that of the basement rocks (Table 2a,b; cf. Jones, 1985a; Koeberl and Reimold, 1996), with a tendency toward granitic compositions, in agreement with petrographic observations. Some of the glasses are enriched in the siderophile elements, including Ir, compared to the average country rocks.

Table 2a. Chemical Composition of Bosumtwi Crater Target Rocks and Suevitic Melt Fragments.

	Shale				Phyllite-Graywacke									Granite Dikes			Pepiakese Granite			Suevitic Melt Fragments			
	J490	J497	J502	J503	J491	J492	J495	J494	J496	J501	J504	J506	B096	J493	J505	B001	J507	J508	J509	B026	B034	B075	B091
SiO_2	53.56	54.31	57.16	57.21	63.30	65.21	69.12	67.66	67.59	67.06	67.32	73.11		68.24	69.24		66.69	53.13	53.60				
TiO_2	0.97	0.88	0.75	0.74	0.77	0.66	0.60	0.67	0.75	0.59	0.61	0.41		0.50	0.50		0.06	0.45	0.88				
Al_2O_3	22.62	19.57	18.39	17.68	17.02	16.26	12.70	14.68	14.85	15.14	16.22	12.29		15.73	16.08		19.87	14.73	14.74				
Fe_2O_3	7.99	9.14	8.77	8.26	6.90	7.57	6.34	6.09	6.26	5.77	5.64	4.23	4.88	4.27	3.66	0.81	0.48	9.17	8.61	4.21	4.57	2.23	9.03
MnO	0.035	0.043	0.051	0.055	0.034	0.031	0.035	0.019	0.031	0.037	0.010	0.026		0.027	0.001		0.001	0.106	0.093				
MgO	2.40	3.31	2.86	3.04	2.44	2.11	2.50	2.09	2.06	1.83	1.79	0.96		1.80	1.09		0.12	10.17	9.60				
CaO	0.05	0.11	0.11	0.08	0.18	0.07	0.17	0.10	0.28	0.47	0.09	1.53		0.32	0.31		0.23	6.76	6.10				
Na_2O	0.62	2.13	0.88	0.36	1.65	0.31	2.88	2.95	2.97	3.07	2.01	4.08	1.99	4.62	3.65	3.45	11.88	2.92	3.31	1.82	2.21	0.01	3.91
K_2O	2.98	3.07	2.64	2.87	2.72	2.32	0.85	1.41	1.52	1.47	2.32	1.31	0.86	1.77	2.08	4.53	0.47	0.27	1.27	1.43	1.18	0.004	0.86
P_2O_5	0.08	0.13	0.06	0.04	0.05	0.02	0.08	0.09	0.10	0.08	0.04	0.10		0.06	0.05		0.02	0.08	0.21				
L.O.I.	7.72	6.86	8.06	8.99	4.81	5.32	4.20	3.71	3.49	4.24	3.96	1.79		2.65	3.31		0.51	2.22	1.70				
Total	99.02	99.56	99.72	99.32	99.86	99.89	99.48	99.46	99.88	99.74	100.00	99.83		99.99	99.97		100.32	100.01	100.11				
Sc	21.9	26.4	22.4	22.9	18.4	18.3	12.5	14.9	14.8	14.3	15.4	7.69	8.74	9.78	9.74	1.23	1.37	27.9	23.3	17.7	14.5	0.91	28.6
V	166	216	160	192	152	141	109	138	129	126	140	118		92	90		33.5	145	150				
Cr	230	183	174	190	167	207	132	150	168	138	190	73.9	39.9	157	96.7	2	19.2	753	779	200	161	5.1	563
Co	18.9	18.2	28.9	24.4	10.4	23.8	6.89	6.14	11.4	13.8	12.5	6.95	17.6	13.4	5.92	0.68	2.95	42.9	45.3	11.9	13.5	1.33	34.1
Ni	58	68	90	101	24	71	37	63	49	45	44	20	14	73	25	6	11	237	267	40	39	16	140
Cu	13.7	84.6	48.5	61.5	15.6	16.7	21.1	12.1	28.7	11.3	3	18.7		3	18.3		3	34	35.9				
Zn	131	145	143	151	115	131	107	97	93	95	92	60	62	86	77	43	6.4	124	139	71	67	9	85
Ga	24	30	18	23	18	19	89	210	67	26	37	36	19	46	27	14	60	70	90	18	23	1	10
As	2.21	14.4	12.7	5.11	0.26	1.02	8.17	15.3	13.2	10.5	0.52	0.55	3.21	27.2	2.56	0.062	19.1	3.22	15.9	4.87	3.12	7.82	5.86
Se	0.15	0.17	0.25	0.18	0.17	0.17	0.22	0.15	0.11	0.18	0.15	0.09	0.06	0.25	0.17	0.05	0.11	0.08	0.09	0.06	0.072	0.04	0.06
Br	0.24	0.26	0.19	0.21	0.12	0.59	0.13	0.13	0.084	0.11	0.11	0.17	0.14	0.17	0.12	0.27	0.21	0.13	0.15	0.28	0.22	0.38	0.04
Rb	114	92.5	102	109	94.5	96.6	25.9	41.5	51.9	56.3	89.8	39.1	19.8	51.2	88.6	335	9.5	7.9	49.9	60.5	42.5	1.2	23.8
Sr	180	149	85	57	145	64	165	172	155	205	155	402	840	311	372	120	335	359	438	190	230	20	390
Y	18	23	22	32	28	13	19	17	13	26	19	10		10	11		5.4	8.5	19				
Zr	163	160	176	114	153	142	119	136	140	158	150	126	57	139	119	96	73	62	110	120	136	20	107
Nb	7.2	6.2	4.0	6.8	6.1	7.4	4.8	4.9	5.3	6.0	5.4	3.0		3.9	3.4		1.6	0.3	3.5				
Ag	0.11	0.07	0.12	0.08	0.08	0.05	0.07	0.11	0.06	0.17	0.04	0.04	0.03	0.15	0.09	0.012	0.05	0.08	0.11	0.07	0.04	0.06	0.05

Table 2a. (Continued)

	Shale				Phyllite-Graywacke									Granite Dikes			Pepiakese Granite			Suevitic Melt Fragments			
	J490	J497	J502	J503	J491	J492	J495	J494	J496	J501	J504	J506	B096	J493	J505	B001	J507	J508	J509	B026	B034	B075	B091
Sb	0.14	0.41	0.59	0.39	0.19	0.16	0.16	0.21	0.17	0.35	0.16	0.16	0.55	0.21	0.14	0.29	0.26	0.64	0.37	0.21	0.16	0.09	1.05
Cs	5.11	3.78	6.42	6.98	3.69	6.03	1.55	2.24	1.78	3.21	4.37	1.98	0.99	2.73	5.71	7.91	0.46	0.63	1.51	2.86	1.84	0.056	0.94
Ba	771	1050	561	677	510	574	265	431	320	515	562	546	320	496	714	260	151	136	391	439	418	40	403
La	16.2	22.1	43.5	41.6	24.6	10.1	30.8	26.9	18.9	36.2	16.1	21.5	10.6	14.8	22.8	7.56	26.3	6.26	14.1	13.2	14.8	0.69	17.9
Ce	21.1	38.1	45.8	48.5	41.7	12.4	33.8	51.6	35.3	42.8	25.8	45.6	13.3	32.1	46.7	17.4	47.2	11.8	37.1	27.5	28.3	1.07	32.8
Nd	13.5	21.8	31.1	46.4	30.1	10.5	38.8	28.5	17.9	42.1	17.6	19.6	5.9	13.4	26.1	7.6	17.5	6.2	28.7	14.7	14.6	0.61	17.5
Sm	3.02	4.39	6.09	8.41	6.47	2.11	6.81	5.64	4.45	6.62	3.35	3.03	0.77	3.49	3.99	1.95	2.91	1.69	6.13	2.45	2.59	0.17	3.96
Eu	0.88	1.12	1.43	2.04	1.22	0.74	1.89	1.31	1.16	1.82	0.86	0.88	0.31	0.89	1.17	0.26	0.83	0.86	1.89	0.77	0.77	0.046	1.11
Gd	3.1	5.1	7.8	10.2	6.4	2	6.7	4.5	3.8	6.8	3.4	3.8	0.7	3.4	3.4	0.92	1.8	2.3	5.1	2.75	2.38	0.18	4.15
Tb	0.56	0.73	1.42	1.51	0.91	0.29	0.99	0.68	0.65	1.11	0.48	0.58	0.11	0.61	0.57	0.15	0.22	0.45	0.75	0.41	0.24	0.045	0.49
Dy	3.7	4.5	7.7	8.4	5.7	2.1	5.6	3.8	3.7	6.4	2.9	3	0.75	3.1	3	0.8	1.3	2.5	4.2	1.9	1.5	0.38	2.9
Tm	0.35	0.39	0.57	0.58	0.51	0.21	0.37	0.31	0.27	0.49	0.27	0.23	0.07	0.24	0.19	0.037	0.1	0.19	0.31	0.14	0.12	0.044	0.23
Yb	2.42	2.63	2.33	3.43	2.84	1.59	2.11	2.15	1.57	2.71	1.98	1.19	0.42	1.08	1.17	0.31	0.55	1.13	1.87	0.61	0.58	0.35	1.51
Lu	0.35	0.37	0.32	0.47	0.38	0.27	0.29	0.29	0.21	0.31	0.25	0.15	0.067	0.16	0.15	0.047	0.075	0.12	0.23	0.09	0.061	0.062	0.23
Hf	4.49	4.28	4.12	3.58	3.71	4.66	3.52	4.34	3.85	4.03	4.14	3.01	2.23	3.54	3.77	1.84	1.84	0.78	3.02	3.29	3.18	0.021	2.33
Ta	0.73	0.52	0.36	0.49	0.55	0.49	0.31	0.37	0.39	0.28	0.58	0.28	0.085	0.19	0.36	0.42	0.11	0.31	0.16	0.22	0.28	0.01	0.21
W	0.55	0.65	0.43	0.38	0.58	0.49	0.48	0.9	0.6	0.56	0.86	0.82	1.56	0.8	0.87	0.17	0.31	0.6	0.7	0.41	0.36	0.061	0.91
Ir (ppb)	<1.5	0.6	<2	<2	<1.5	<1.5	<1.5	<1.5	<1.5	<2	<1.5	<1	0.2	<1.5	<2	0.1	<1	<1	<1	0.3	0.2	<0.5	0.8
Au (ppb)	7.5	10.5	9	20	10	13	10	13	8	11	7	33	2.2	25	18	0.6	17	10	28	10.8	0.6	0.8	2.2
Hg	<0.1	<0.08	0.08	0.06	<0.1	0.09	0.12	<0.08	0.09	<0.1	<0.08	0.12	0.06	0.06	0.05	0.03	0.08	<0.1	<0.1	0.05	0.05	0.09	0.03
Th	4.48	4.23	4.37	4.34	4.15	4.46	2.99	3.81	3.29	4.47	4.42	2.93	0.79	2.83	3.37	1.86	5.17	0.71	0.75	3.55	3.27	0.024	2.11
U	1.67	1.81	1.85	1.43	1.39	1.23	1.38	1.47	1.18	1.62	1.19	0.75	0.23	1.86	1.64	3.61	1.47	0.23	0.53	1.01	0.63	0.082	0.35
K/U	14885	14134	11892	16713	16331	15738	5145	7976	10734	7541	16254	14556	31159	7930	10559	10457	2647	9783	19969	11799	15608	407	20476
Zr/Hf	36.3	37.4	42.7	31.8	41.2	30.5	33.8	31.3	36.4	39.2	36.2	41.9	25.6	39.3	31.6	52.2	39.7	79.5	36.4	36.5	42.8	952.4	45.9
La/Th	3.62	5.22	9.95	9.59	5.93	2.26	10.30	7.06	5.74	8.10	3.64	7.34	13.42	5.23	6.77	4.06	5.09	8.82	18.80	3.72	4.53	28.75	8.48
Hf/Ta	6.15	8.23	11.44	7.31	6.75	9.51	11.35	11.73	9.87	14.39	7.14	10.75	26.24	18.63	10.47	4.38	16.73	2.52	18.88	14.95	11.36	2.10	11.10
Th/U	2.68	2.34	2.36	3.03	2.99	3.63	2.17	2.59	2.79	2.76	3.71	3.91	3.43	1.52	2.05	0.52	3.52	3.09	1.42	3.51	5.19	0.29	6.03
La_N/Yb_N	4.52	5.68	12.62	8.20	5.85	4.29	9.86	8.45	8.13	9.03	5.49	12.21	17.05	9.26	13.17	16.48	32.31	3.74	5.10	14.62	17.24	1.33	8.01
Eu/Eu*	0.88	0.72	0.63	0.67	0.58	1.10	0.86	0.79	0.86	0.83	0.78	0.79	1.29	0.79	0.97	0.59	1.11	1.33	1.03	0.91	0.95	0.80	0.84

Major element data in wt%, trace element data in ppm, except as noted. All Fe as Fe_2O_3. Blank spaces: not determined.

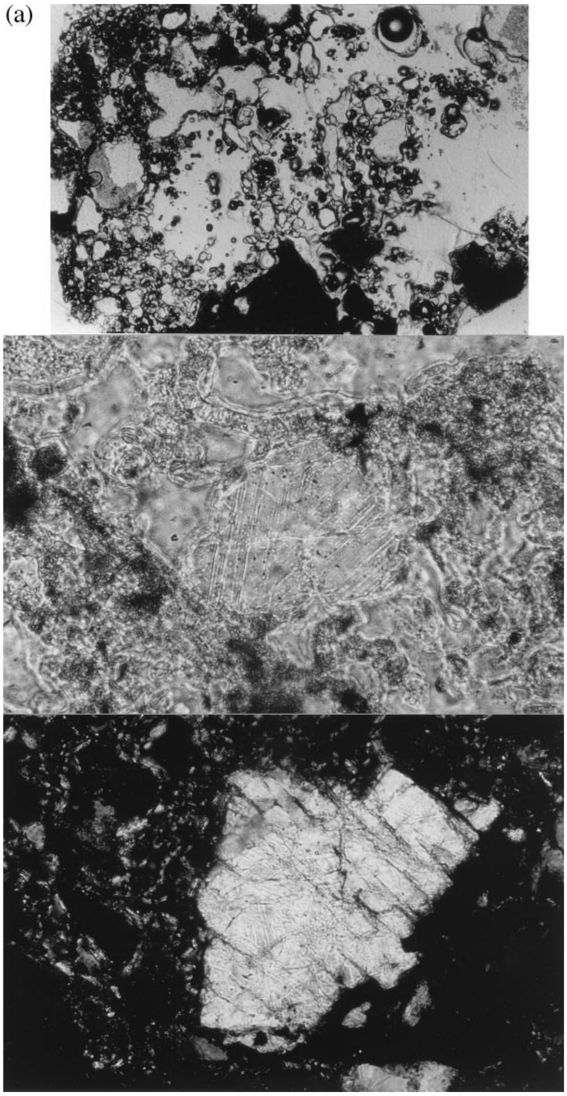

Fig. 6. Photomicrographs of melt fragments from suevitic breccias from the Bosumtwi crater. (a) Vesicular glass from melt fragment in suevite, with flow structure; sample B075, 3.4 mm wide, plane polarized light. (b) Quartz clasts with at least two sets of PDFs in altered micaceous matrix, possibly from quartzite or graywacke precursor, sample B034, 85 μm wide, plane polarized light. (c) Quartz clast within melt fragment from suevite, with multiple sets of PDFs, sample B034, 355 μm wide, crossed polarizers.

3.3. Isotopic Data

The $\delta^{18}O$ values (Table 3) of the analyzed shale, graywacke, and phyllite fall in the narrow range of 11.3 to 13.2‰, typical of clastic sedimentary rocks (Taylor and Sheppard, 1986). The two samples of granite dikes and three samples of the Pepiakese granite have a much wider range of values. The granite dikes have values $\delta^{18}O$ of 12.7 and 12.9‰, which are identical to the surrounding sedimentary rocks and typical of anatectic granites. The Pepiakese granite samples have values of 8.6 to 9.0‰, which are more typical of either primitive mantle-derived magmatic rocks or anatectic granites subjected to meteoric-hydrothermal alteration. The two samples of suevite have $\delta^{18}O$ values of 12.6 and 12.9‰, consistent with their derivation from the sedimentary rocks or granite dikes.

ϵ_{Nd} is the measured deviation in parts in 10^4 of the $^{143}Nd/^{144}Nd$ ratio from the present-day chondritic uniform reservoir (CHUR) value of 0.512638, and ϵ_{Sr} is the measured deviation in parts in 10^4 of the $^{87}Sr/^{86}Sr$ ratio from the inferred unfractionated terrestrial mantle reservoir (UR) reference value of 0.7045. Depleted mantle Nd model ages (T_{DM}; also known as mantle separation ages) are a calculation of the time that a sample last had the isotopic composition of a depleted mantle model reservoir (DePaolo, 1981) and are also given in Table 3. $^{87}Sr/^{86}Sr$ and Rb/Sr ratios vary considerably among the target rocks with $^{87}Sr/^{86}Sr$ ranging from 0.70285 to 0.755285 and Rb/Sr ranging from 0.0220 to 0.652. When plotted on a Rb-Sr isotope evolution diagram (Fig. 8) it is evident that the samples plot along a general trend, but scatter considerably about a best-fit line due to the fact that (1) the various rock types probably do not have identical ages or initial $^{87}Sr/^{86}Sr$ ratios, and (2) many of the rocks are considerably altered. Nevertheless, an "isochron" was fit to the target rock analyses using the method of York (1969) and yields a best fit "age" of 1.98 Ga and initial $^{87}Sr/^{86}Sr$ ratio of 0.701; this line is shown on Fig. 8 for reference, but cannot be considered a reliable age of deposition or crystallization for these rocks. This is a similar result to several earlier studies of the Rb-Sr isotope systematics of Bosumtwi crater target rocks (Schnetzler et al., 1966; Lippolt and Wasserburg, 1966; Kolbe et al., 1967). The "age" and initial $^{87}Sr/^{86}Sr$ ratio also compare favorably with more recent studies of the Rb-Sr geochronology of Birimian granitoids, which yielded isochrons with ages of 1.82 to 2.22 Ga and initial $^{87}Sr/^{86}6Sr$ ratios of 0.701 to 0.704 (Taylor et al., 1992). A plot of $^{87}Sr/^{86}Sr$ vs. $\delta^{18}O$ (Fig. 9) graphically portrays the wide range of $^{87}Sr/^{86}Sr$ and narrow range of $\delta^{18}O$ of the sedimentary rocks and granite dikes, and the contrasting low $^{87}Sr/^{86}Sr$ and $\delta^{18}O$ values of the Pepiakese granite.

Three samples of sedimentary target rocks, one sample of the Pepiakese granite, and two samples of suevitic melt were analyzed for $^{143}Nd/^{144}Nd$ ratios and have ϵ_{Nd} values ranging from -17.2 to -25.9. These values have a similar range as that previously measured for Birimian sediments and granitoids (Taylor et al., 1992). Depleted mantle Nd model ages were calculated for the sedimentary target rocks and range from 2.16 to 2.64 Ga, which is also similar to the model ages ranging from 2.01 to 2.62 previously measured for Birimian sediments and granitoids (Taylor et al., 1992). Pb-Pb and Sm-Nd whole rock isochron ages for Birimian granitoids range from 1.97 to 2.18 Ga, and U-Pb ages on detrital zircons from Birimian sediments yield ages of 2.14 to 2.18 Ga (Davis et al., 1994). The close correspondence of the Nd model ages with the granitoid crystallization ages suggest that the granitoids and volcanics that contributed detritus to the sediments were probably derived from the depleted mantle source region within the 2.0 to 2.6 Ga time interval.

3.4. Comparison of Bosumtwi Crater Rocks with Ivory Coast Tektites

Several lines of argument link the Bosumtwi crater with the formation of the Ivory Coast tektites. Previously published age data for both the Bosumtwi crater and the Ivory Coast tektites

Table 2b. Average and range of Compositions of Bosumtwi Crater Target Rocks, Impact Glass, and Ivory Coast Tektites.

	Shale		Graywacke - Phyllite		Granite Dike	Pepiakese Granite		Impact Glass	Tektites
	Average	Range	Average	Range	Average	Average	Range	BI9201	Average
SiO_2	55.56±1.65	53.56 - 57.21	66.75±1.77	63.30 - 69.12	68.74±0.50	57.81±6.28	53.13 - 66.69		67.58
TiO_2	0.84±0.10	0.74 - 0.97	0.66±0.07	0.59 - 0.77	0.50±0.00	0.46±0.34	0.06 - 0.88		0.56
Al_2O_3	19.56±1.89	17.68 - 22.62	15.27±1.31	12.70 - 17.02	15.91±0.18	16.45±2.42	14.73 - 19.87		16.74
Fe_2O_3	8.54±0.45	7.99 - 9.14	6.37±0.62	5.64 - 7.57	3.97±0.31	6.09±3.97	0.48 - 9.17	6.65	6.16
MnO	0.046±0.008	0.035 - 0.055	0.028±0.009	0.010 - 0.037	0.014±0.013	0.067±0.047	0.001 - 0.106		0.06
MgO	2.90±0.34	2.40 - 3.31	2.12±0.25	1.79 - 2.50	1.44±0.36	6.63±4.61	0.12 - 10.17		3.46
CaO	0.09±0.02	0.05 - 0.11	0.19±0.13	0.07 - 0.47	0.31±0.01	4.36±2.94	0.23 - 6.76		1.38
Na_2O	1.00±0.68	0.36 - 2.13	2.26±0.95	0.31 - 3.07	4.14±0.49	6.04±4.14	2.92 - 11.88	3.73	1.90
K_2O	2.89±0.16	2.64 - 3.07	1.80±0.61	0.85 - 2.72	1.92±0.15	0.67±0.43	0.27 - 1.27	1.51	1.95
P_2O_5	0.08±0.03	0.04 - 0.13	0.06±0.03	0.02 - 0.10	0.06±0.00	0.10±0.08	0.02 - 0.21		
L.O.I.	7.91±0.76	6.86 - 8.99	4.25±0.59	3.49 - 5.32	2.98±0.33	1.48±0.71	0.51 - 2.22		0.002
Total	99.41		99.76		99.98	100.15			99.79
Sc	23.4±1.8	21.9 - 26.4	15.5±2.0	12.5 - 18.4	9.76±0.02	17.5±11.6	1.37 - 27.9	17.1	14.7
V	184±22	160 - 216	134±13	109 - 152	91±1	110±54	33.5 - 150		
Cr	194±21	174 - 230	165±25	132 - 207	127±30	517±352	19.2 - 779	280	244
Co	22.6±4.4	18.2 - 28.9	12.1±5.4	6.14 - 23.8	9.66±3.74	30.4±19.4	2.95 - 45.3	24.5	26.7
Ni	79±17	58 - 101	48±15	24 - 71	49±24	172±114	11 - 267	99	157
Cu	52±26	13.7 - 84.6	15.5±7.5	3 - 28.7	10.7±7.7	24.3±15.1	3 - 35.9		
Zn	143±7	131 - 151	104±13	92 - 131	82±5	90±59	6.4 - 139	138	23
Ga	24±4	18 - 30	67±63	18 - 210	37±10	73±12	60 - 90	45	21
As	8.61±5.09	2.21 - 14.4	7.00±5.91	0.26 - 15.3	14.9±12.3	12.7±6.9	3.22 - 19.1	4.59	0.45
Se	0.19±0.04	0.15 - 0.25	0.16±0.03	0.11 - 0.22	0.21±0.04	0.09±0.01	0.08 - 0.11	0.14	0.23
Br	0.23±0.03	0.19 - 0.26	0.18±0.17	0.084 - 0.59	0.15±0.03	0.16±0.03	0.13 - 0.21	1.06	0.79
Rb	104±8	92.5 - 114	65.2±26.2	25.9 - 96.6	69.9±18.7	22.4±19.4	7.9 - 49.9	36.6	66
Sr	118±49	57 - 180	152±40	64 - 205	342±31	377±44	335 - 438	389	260
Y	23.8±5.1	18 - 32	19±5	13 - 28	11±1	11±6	5.4 - 19		
Zr	153±23	114 - 176	143±12	119 - 158	129±10	82±21	62 - 110	140	134
Nb	6.1±1.2	4.0 - 7.2	5.7±0.8	4.8 - 7.4	3.7±0.3	1.8±1.3	0.3 - 3.5		
Ag	0.10±0.02	0.07 - 0.12	0.08±0.04	0.04 - 0.17	0.12±0.03	0.08±0.02	0.05 - 0.11	0.25	0.1
Sb	0.38±0.16	0.14 - 0.59	0.20±0.06	0.16 - 0.35	0.18±0.04	0.42±0.16	0.26 - 0.64	0.36	0.23
Cs	5.57±1.24	3.78 - 6.98	3.27±1.48	1.55 - 6.03	4.22±1.49	0.87±0.46	0.46 - 1.51	2.21	3.67
Ba	765±181	561 - 1050	454±112	265 - 574	605±109	226±117	136 - 391	609	327
La	30.9±11.9	16.2 - 43.5	23.4±8.3	10.1 - 36.2	18.8±4.0	15.6±8.2	6.26 - 26.3	18.9	20.7
Ce	38.4±10.7	21.1 - 48.5	34.8±11.8	12.4 - 51.6	39.4±7.3	32.0±14.9	11.8 - 47.2	39.2	41.9
Nd	28.2±12.2	13.5 - 46.4	26.5±10.8	10.5 - 42.1	19.8±6.4	17.5±9.2	6.2 - 28.7	18.5	21.8
Sm	5.48±2.01	3.02 - 8.41	5.06±1.68	2.11 - 6.81	3.74±0.25	3.58±1.87	1.69 - 6.13	3.59	3.95
Eu	1.37±0.43	0.88 - 2.04	1.29±0.41	0.74 - 1.89	1.03±0.14	1.19±0.49	0.83 - 1.89	1.16	1.2
Gd	6.55±2.69	3.1 - 10.2	4.80±1.73	2 - 6.8	3.40±0.00	3.07±1.45	1.8 - 5.1	4.1	3.34
Tb	1.06±0.42	0.56 - 1.51	0.73±0.27	0.29 - 1.11	0.59±0.02	0.47±0.22	0.22 - 0.75	0.71	0.56
Dy	6.08±2.01	3.7 - 8.4	4.31±1.49	2.1 - 6.4	3.05±0.05	2.67±1.19	1.3 - 4.2	3.6	3.48
Tm	0.47±0.10	0.35 - 0.58	0.35±0.11	0.21 - 0.51	0.22±0.03	0.20±0.09	0.1 - 0.31	0.24	0.30
Yb	2.70±0.43	2.33 - 3.43	2.14±0.46	1.57 - 2.84	1.13±0.05	1.18±0.54	0.55 - 1.87	1.39	1.79
Lu	0.38±0.06	0.32 - 0.47	0.29±0.05	0.21 - 0.38	0.16±0.01	0.14±0.07	0.075 - 0.23	0.20	0.24
Hf	4.12±0.34	3.58 - 4.49	4.04±0.36	3.52 - 4.66	3.66±0.12	1.88±0.91	0.78 - 3.02	4.98	3.38
Ta	0.53±0.13	0.36 - 0.73	0.42±0.11	0.28 - 0.58	0.28±0.09	0.19±0.08	0.11 - 0.31	0.48	0.34
W	0.50±0.11	0.38 - 0.65	0.64±0.16	0.48 - 0.90	0.84±0.04	0.54±0.17	0.31 - 0.7	0.6	0.63
Au (ppb)	11.8±4.9	7.5 - 20	10.3±2.1	7 - 13	21.5±3.5	18.3±7.4	10 - 28	31	56
Hg	0.04±0.04	0.01 - 0.08	0.04±0.05	0.01 - 0.12	0.06±0.01	0.03±0.04	0.01 - 0.08	0.08	0.28
Th	4.36±0.09	4.23 - 4.48	3.94±0.56	2.99 - 4.47	3.10±0.27	2.21±2.09	0.71 - 5.17	4.22	3.54
U	1.69±0.16	1.43 - 1.85	1.35±0.15	1.18 - 1.62	1.75±0.11	0.74±0.53	0.23 - 1.47	1.44	0.94
K/U	14406±1728	11892 - 16713	11389±4357	5145 - 16331	9245±1314	10800±7108	2647 - 19969	8738	17287
Zr/Hf	37.1±3.9	31.8 - 42.7	35.5±3.7	30.5 - 41.2	35.4±3.9	51.9±19.6	36.4 - 79.5	28.1	39.6
La/Th	7.10±2.74	3.62 - 9.95	6.15±2.49	2.26 - 10.30	6.00±0.77	10.90±5.79	5.09 - 18.80	4.48	5.85
Hf/Ta	8.28±1.97	6.15 - 11.44	10.11±2.48	6.75 - 14.39	14.55±4.08	12.71±7.26	2.52 - 18.88	10.38	9.94
Th/U	2.60±0.28	2.34 - 3.03	2.95±0.51	2.17 - 3.71	1.79±0.27	2.67±0.91	1.42 - 3.52	2.93	3.77
La_N/Yb_N	7.75±3.11	4.52 - 12.62	7.30±1.93	4.29 - 9.86	11.21±1.95	13.72±13.16	3.74 - 32.31	9.19	7.81
Eu/Eu*	0.73±0.09	0.63 - 0.88	0.83±0.14	0.58 - 1.10	0.88±0.09	1.16±0.13	1.03 - 1.33	0.92	1.01

Major element data in wt%, trace element data in ppm (except as noted); all Fe as Fe_2O_3. Ivory Coast tektite data from Koeberl et al. (1997a).

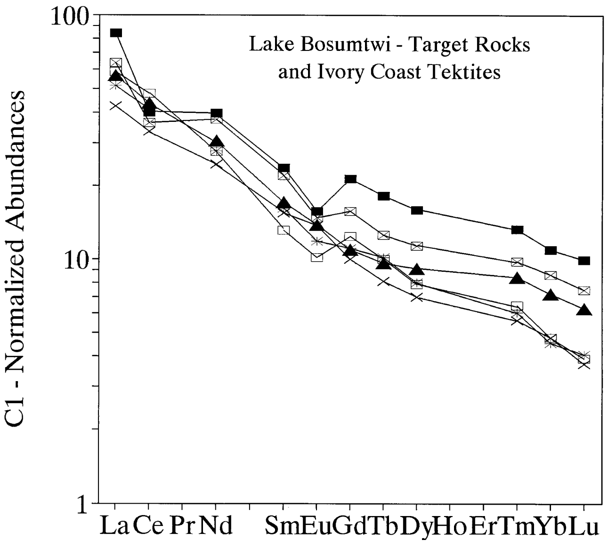

Fig. 7. Average and chondrite-normalized rare earth element distribution patterns for the various Bosumtwi crater rocks (this work) and Ivory Coast tektites (Koeberl et al., 1997a). Normalization factors from Taylor and McLennan (1985, p. 298). Symbols: -■-, shale; -⊠-, graywacke-phyllite; -✳-, granite dikes, -⊟-, graywacke; -✕-, pepiakese granite; -▲-, avg. IVC-tektite.

range from about 0.7 to 1.3 Ma (e.g., Zähringer, 1963; Fleischer et al., 1965; Gentner et al., 1969a,b; Durrani and Khan, 1971; Bollinger, 1993). Most recently, Koeberl et al. (1997a) reported on ^{40}Ar-^{39}Ar dating of Ivory Coast tektites, yielding an age of 1.1 $\pm$ 0.05 Ma, and an average fission-track age of 1.05 $\pm$ 0.11 Ma, which is, within errors, identical to the age of the Bosumtwi impact glass at 1.03 $\pm$ 0.11 Ma, with a preferred age of the impact event at 1.07 Ma.

Furthermore, the distribution and stratigraphic age of Ivory Coast microtektites also help to constrain the age of the event and the relation with the Bosumtwi crater. Glass and Pizzuto (1994) studied microtektite abundances in deep sea cores and related the ejecta thickness to distance from the source crater. They were able to show that the amount of microtektites in the deep-sea cores increases towards the Bosumtwi crater, and that a source crater calculated from empirical equations has a diameter of 12.6 $\pm$ 3.4 km, which is in good agreement with the actual size of the Bosumtwi crater. Durrani and Khan (1971) and Glass et al. (1979) suggested that the Ivory Coast tektite event and the onset of the Jaramillo geomagnetic reversal might be related, but Schneider and Kent (1990) and Glass et al. (1991) showed that the microtektites were deposited about 8000 years after the onset of the Jaramillo subchron, which was dated at 1.07 Ma (Cande and Kent, 1995). Thus, the magnetostratigraphic age of the Ivory Coast microtektites (1.06 Ma) is in very good agreement with the tektite and impact glass ages derived by Koeberl et al. (1997a).

Several authors (e.g., Schnetzler et al., 1966, 1967; Koeberl et al., 1997a) have concluded that the chemical composition of the Ivory Coast tektites is in agreement with their derivation from about 2 Ga old Archean crustal rocks, which would agree with the ages of the rocks at Lake Bosumtwi. The Ivory Coast tektites have negative ϵ_{Nd} values of about -20 (Shaw and Wasserburg, 1982; this work), and yield depleted mantle Nd model ages of about 2.1 Ga (Table 3), which is in agreement with the whole rock Rb-Sr ages of the rocks around the Bosumtwi crater (see below). Chamberlain et al. (1993) found that the oxygen isotopic characteristics of the tektites are almost indistinguishable from those of the sedimentary country rocks around Bosumtwi (see also below). The B isotopic composition of Ivory Coast tektites, with low B abundances and slightly negative $\delta^{11}B$ values, are also consistent with granitic and metasedimentary source rocks (Chaussidon and Koeberl, 1995).

Ivory Coast tektites are very homogeneous with respect to their major and trace element composition (e.g., Gentner et al., 1964; Schnetzler et al., 1966, 1967; Pinson and Griswold, 1969; Rybach and Adams, 1969; Chapman and Scheiber, 1969; Cuttitta et al., 1972; Koeberl et al., 1997a). However, in contrast to tektites from other strewn fields, Ivory Coast tektites have relatively high contents of Cr, Co, and Ni (e.g., Chapman and Scheiber, 1969; Cuttitta et al., 1972; Koeberl et al., 1987), as well as for Ir and some other siderophile elements (Palme et al., 1978). Palme et al. (1978, 1981) proposed that these high siderophile element contents could be due to an extraterrestrial component. In contrast, Jones (1985a) suggested that high indigenous contents of the target rocks at Bosumtwi could be the source for these elements in the tektites. Data by Koeberl et al. (1997a) on Ivory Coast tektites show highly variable Au contents between 1.6 and 89 ppb, which are not accompanied by comparably high Ir values. However, Koeberl and Shirey (1993) determined the abundances and isotopic ratios of Os and Re in Ivory Coast tektites and Bosumtwi crater rocks, and, while the Os abundances in the Bosumtwi rocks can be high (0.02–0.33 ppb), the $^{187}Os/^{188}Os$ ratios of the tektites (0.153–0.209) are within the meteoritic range, while Bosumtwi crater target rocks were found to have $^{187}Os/^{188}Os$ ratios that are typical for old continental crust. A meteoritic contribution to the tektites not exceeding 0.05–0.1 wt% was estimated by Koeberl and Shirey (1993). These authors also concluded that the isotopic composition of the tektites in the $^{187}Os/^{188}Os$ and $^{187}Re/^{188}Os$ diagram can best be explained by mixing of Os from Bosumtwi country rocks with meteoritic Os, providing another link between Ivory Coast tektites and the Bosumtwi impact crater.

A direct comparison of the compositions of the Bosumtwi target rocks with Ivory Coast tektites (Table 2b) shows some similarities. The major element composition of the tektites is, for most elements, similar to that of the average graywacke-phyllite, with the exception of slightly higher Mg, and significantly higher Ca contents in the tektites. Jones (1985a) averaged all his Bosumtwi rock analyses and compared them with the average tektite compositions, and also noted the discrepancy in Ca and Mg contents. He concluded that admixture of about 25–30% Pepiakese granite would provide a more adequate result. However, the isotopic data (Table 3, and below) do not seem to allow for such a high contribution.

The Ivory Coast tektite REE patterns show high absolute abundances and steep patterns without any prominent Eu anomaly (Fig. 7). These patterns are very similar to those of the rocks from the Bosumtwi crater. As shown in Fig. 7, the granite dike and the graywacke-phyllite patterns are very similar to that of the average tektites. No Ce anomalies, such as those displayed by the mylonitized and strongly altered shales and

Table 3. Isotopic data and calculated parameters for isotopic evolution.

Sample	$\delta^{18}O$	Rb/Sr	$^{87}Sr/^{86}Sr$ (±2σ)	ε_{Sr}	Sm/Nd	$^{143}Nd/^{144}Nd$ (±2σ)	ε_{Nd}	T_{DM} (Nd)
Ivory Coast Tektites								
IVC 2069	11.7	0.265	0.723763 (19)	273	0.187	–	–	–
IVC 2113	12.6	–	–	–	–	–	–	–
IVC 3395	12.7	–	–	–	–	–	–	–
IVC 3396	12.9	0.268	0.722292 (18)	252	0.215	–	–	–
IVC 3398	12.0	0.225	0.722132 (22)	250	0.179	0.511583 (21)	-20.6	2.11
†USNM6011A	–	0.216	0.72334 (3)	267	0.188	–	-20.2	2.20
†USNM6011B	–	0.224	0.72357 (4)	270	–	–	–	–
†USNM6011C	–	0.271	0.72571 (3)	301	0.188	–	-19.5	2.16
Suevite								
BCC-5A-64	12.9	–	0.718064 (20)	192	–	0.511755 (20)	-17.2	–
BCC-8A-64	12.6	–	0.717493 (20)	184	–	0.511601 (20)	-20.2	–
Shale								
J490	13.2	0.633	0.755285 (17)	720	0.224	0.511691 (24)	-18.5	2.64
J497	12.5	0.621	0.742688 (13)	542	0.201	–	–	–
Phyllite and Graywacke								
J491	13.1	0.652	0.750069 (20)	646	0.215	0.511661 (20)	-19.1	2.54
J494	12.9	0.241	0.722356 (11)	253	0.198	–	–	–
J495	11.3	0.157	0.714000 (19)	134	0.176	–	–	–
J501	13.6	0.275	0.729800 (20)	359	0.157	0.511360 (20)	-24.9	2.16
J506	12.6	0.0973	0.706011 (11)	21.5	0.155	–	–	–
Granite Dikes								
J493	12.7	0.165	0.711833 (35)	104	0.260	–	–	–
J505	12.9	0.238	0.720106 (14)	221	0.153	–	–	–
Pepiakese Granite								
J507	9.0	0.0284	0.703523 (27)	-13.8	0.166	0.511309 (14)	-25.9	2.33
J508	8.6	0.0220	0.702850 (10)	-23.4	0.273	–	–	–
J509	8.8	0.114	0.709259 (11)	67.6	0.214	–	–	–

†Data from Shaw and Wasserburg (1982). Rb/Sr = elemental abundance ratio. 2σ uncertainties refer to the last digits of the measured isotope ratio. ε values are the measured deviation in parts in 10^4 of the $^{143}Nd/^{144}Nd$ ratio from the present-day chrondritic uniform reservoir (CHUR) value of 0.512638, and of the $^{87}Sr/^{86}Sr$ ratio from the inferred unfractionated mantle reservoir (UR) reference value of 0.7045. T_{DM} is the depleted mantle Nd model age and is a calculation of the time that each sample last had the isotopic composition of the depleted mantle model reservoir given by DePaolo (1981).

graywackes (Fig. 7), were found in any of the tektite samples. The suevite-derived melt fragments have abundances of the REE and other trace elements that are similar to those of a small impact glass fragment (which was probably also derived from suevite; cf. Gentner, 1966; El Goresy, 1966; Gentner et al., 1967; Koeberl et al., 1997a).

To obtain some constraints on the rocks that might have been melted to form the Ivory Coast tektites, we performed mixing calculations, using average compositions of the four major rock types present at the Bosumtwi crater. We employed the harmonic least-squares (HMX) mixing calculation program (Stöckelmann and Reimold, 1989), which allows the variation of any number of target rock components and mixture parameters (e.g., elemental abundances) as well as inclusion of uncertainties. Not all chemical data are useful for mixing calculations. For example, the highly mobile alkali elements are not commonly useful in these calculations. In the present case, a variety of major and trace element parameters were evaluated.

As endmembers for the calculations, four target rock components were used: shale, phyllite-graywacke, granite dike, and Pepiakese granite. For the first three, average compositions (with standard deviations), as given in Table 2b, were used. Due to the significant variations in composition between the three Pepiakese granite samples, only one of them (J508) was used for an endmember composition, probably being representative of a weathered surface rock with relatively high Ca and Mg contents. The average Ivory Coast tektite composition (from Koeberl et al., 1997a) was used as the ideal result of the calculations and is given in Table 2b. The best results of the mixing calculations are presented in Table 4. The calculated mixture compositions, and deviations of the calculated from the observed values, are given in Table 5. Discrepancy factors listed in Table 4 are a calculated measure for the validity of the results: the better and statistically more valid a result, the closer the corresponding discrepancy value approaches 0 (see Stöckelmann and Reimold, 1989, for details). All calculations given in Tables 4 and 5 have good discrepancy factors. If seven major elements (including the mobile K and the probably weathering-

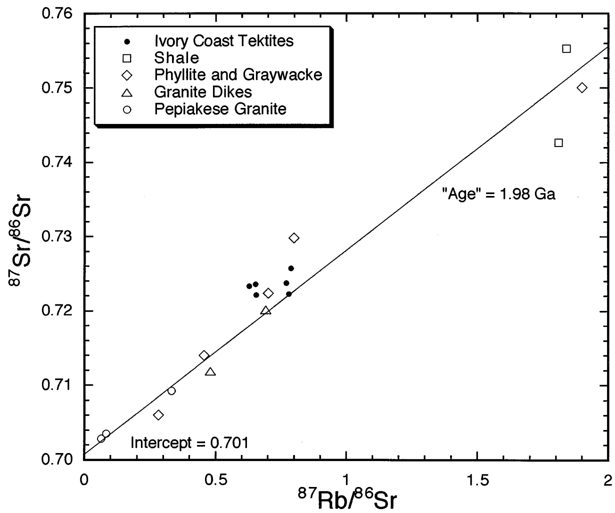

Fig. 8. Rb-Sr isotope evolution diagram for Ivory Coast tektites and Bosumtwi crater target rocks from this study and Shaw and Wasserburg (1982). The isochron for the target rocks only is shown for reference but is not intended to represent a precise age of these sediments or granites (see text).

dependent Ca) are included in the calculations (run 1), the mixture includes only two components, phyllite-graywacke and Pepiakese granite at about 83 to 17%, respectively. Exclusion of K (run 2), and K and Ca (run 3) yields a decrease in the phyllite-graywacke component, and inclusion of a granite dike component, with a slight decrease of the Pepiakese component. Inclusion of various immobile (lithophile) trace elements in the calculations result in very similar mixtures, with about 70% phyllite-graywacke, 16% granite dike, and 14% Pepiakese granite, and <2.5% shale. The results reproduce the observed compositions very well, with the highest deviations observed for those elements that show the largest standard deviations from an average (which in harmonic least-squares analysis is not trivia, as errors of both components and mixtures are taken into account).

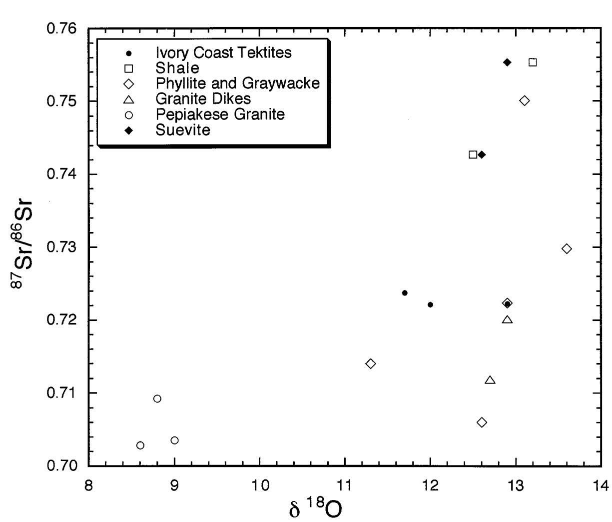

Fig. 9. $^{87}Sr/^{86}Sr$ vs. $\delta^{18}O$ for Ivory Coast tektites and Bosumtwi crater suevitic melt fragments and target rocks from this study.

Using the isotopic compositions of the target rocks and Ivory Coast tektites in addition to the major and trace element chemistry, we can test the widely held view that the composition of tektites from a given strewn field should represent a homogenized mixture of rocks exposed near the surface in the area of impact (e.g., Koeberl, 1994). For Ivory Coast tektites, this assumption is supported by ^{10}Be data of Tera et al. (1983a,b). To examine this assumption and perhaps assess the proportion that each target rock contributed to the tektites, we have taken data for the O, Sr, and Nd isotopic composition of Ivory Coast tektites from the literature (Shaw and Wasserburg, 1982; Taylor and Epstein, 1966), added additional analyses as a part of this study (Table 3), and plotted them together on Figs. 8–11. Because all of the target rocks plot near a single regression line (Fig. 8), any mixture of these rocks will also plot near that line.

Six samples of Ivory Coast tektites cluster within a narrow range of compositions near to the regression line as expected. Although there is a rather narrow range of Sr concentrations of the target rocks (145–438 ppm) and tektites (190–350 ppm), we have plotted $^{87}Sr/^{86}Sr$ vs. 1/Sr for all of the samples on Fig. 10 to evaluate possible mixing relations, which should fall along lines on such a diagram. The basic observation here is that the composition of the target rocks is so variable that distinct endmembers cannot be unambiguously defined. The tektites plot near the center of the cluster of target rock compositions, but it cannot be ascertained whether they are a mixture of sedimentary rocks with $^{87}Sr/^{86}Sr$ of about 0.725 and variable Sr concentration, or are a mixture of granites with lower $^{87}Sr/^{86}Sr$ with sediments with much higher $^{87}Sr/^{86}Sr$.

The range of $\delta^{18}O$ for Ivory Coast tektites that we measured is 11.7 to 12.9‰, whereas Taylor and Epstein (1966) measured somewhat higher values of 12.8 to 14.6‰. Thus, the range for the tektites is very close to the range for sediments and granite dikes. On a plot of $^{87}Sr/^{86}Sr$ vs. $\delta^{18}O$ (Fig. 9), mixtures of source materials should also plot along mixing lines. This diagram is somewhat more telling in that it shows that the tektites are predominantly a mixture of sediments (and possibly granite dikes) with the possibility of only a minor contribution from the Pepiakese granite. The amount of Pepiakese granite obtained from the major and trace element mixing calculations is at the upper limit of the contribution allowed from the isotopic data.

An additional source of oxygen that may be important as an endmember for tektites is admixture of interstitial meteoric water. The lowering of $\delta^{18}O$ values of impact melt rocks relative to their parent target materials has been observed for Central European tektites (moldavites), where a direct link has been established between target material and impact melt rock. Central European tektites are believed to have been produced by melting of the Miocene surficial sands from the Ries crater, yet the tektites have $\delta^{18}O$ values 4.5‰ lower than the values for the target material (Engelhardt et al., 1987). This difference has been explained for the moldavites by the impact-induced admixture of about 25% isotopically light meteoric water that is presumed to have been present in the pore spaces of the target sandstones (Engelhardt et al., 1987). The Australasian tektites ($\delta^{18}O$ values of 9 to 11‰) are proposed to have been derived from Jurassic sandstone and shale (Blum et al., 1992), which

Table 4. Results of Harmonic Least Squares Mixing (HMX) Calculations to Reproduce Ivory Coast Tektite Compositions From Bosumtwi Crater Rocks

	Target Rock Components				Discrepancy
Run	Shale	Phyllite-Graywacke	Granite Dike	Pepiakese Granite	Factor
1 (Si, Ti, Al, Fe, Mg, Ca, K)	0±1.9	83.3±3.7	0±2.0	16.7±1.2	1.18
2 (Si, Ti, Al, Fe, Mg, Ca)	0±1.9	63.3±7.0	19.5±6.0	17.2±1.3	1.33
3 (Si, Ti, Al, Fe, Mg)	0±2.3	72.1±7.7	13.7±5.9	14.2±2.4	1.11
4 (as 3, + Sc, Rb, Zr)	0±0.6	71.6±5.6	15.1±4.6	13.3±1.9	1.25
5 (as 4, + Hf, Th)	0±0.5	70.5±4.7	15.8±4.0	13.7±1.6	1.33
6 (as 5, + La, Yb)	0±0.5	70.0±4.1	16.2±3.6	13.8±1.4	1.33

Components were forced to total 100%. Mixing proportions given in %. Elements listed in parentheses are those used in the mixing calculations of the respective runs.

would be expected to have had original $\delta^{18}O$ values of ~14‰, yet the observed values are about 4‰ lower (Taylor and Epstein, 1969), perhaps also because of meteoric water incorporation (Blum and Chamberlain, 1992). Finally, it is likely that impact-induced admixture of pore water in the Manson (Iowa, USA) crater target rocks (in particular the sandstones) could have provided an additional endmember responsible for the observed ~3‰ lowering of the $\delta^{18}O$ value of melt rock found in the crater relative to the silicate target rocks (Blum et al., 1996). The agreement in the $\delta^{18}O$ values of the Bosumtwi target rocks (except for the Pepiakese granite) and both the Ivory Coast tektites and Bosumtwi suevite suggest that meteoric water incorporation was probably not an important process in the Bosumtwi impact, although some of the variability in the values for the tektites could reflect minor water incorporation.

It was first demonstrated by Shaw and Wasserburg (1982) that tektites from each known strewn field have narrow and distinct ranges of ϵ_{Sr} and ϵ_{Nd} and this observation can be used as a test of whether a particular tektite belongs to a particular strewn field (Blum et al., 1992; Glass et al., 1995). ϵ_{Sr} and ϵ_{Nd} values for each of the known strewn fields are plotted on Fig. 11 and define four distinct regions. As in the case of Sr isotope values, the Nd isotope values of the Bosumtwi target rocks are highly variable. The narrow range of values for the Ivory Coast tektites falls in the center of the range of target rock values suggesting that the tektite production process may homogenize and average heterogeneous target rock compositions. The Bosumtwi Crater suevitic melt samples are closer to, but not within, the Ivory Coast tektite field, suggesting that they preserve heterogeneities in the target rock compositions, which is in agreement with our petrographic observations of numerous target rock derived clasts in these melt fragments.

4. SUMMARY AND CONCLUSIONS

The Bosumtwi crater, located in Ghana in West Africa, has a rim to rim diameter of 10.5 km and is almost completely filled by Lake Bosumtwi. The crater has been known since last

Table 5. Comparison of Measured Ivory Coast Tektite Compositions with those Obtained from the Mixing Calculations using Bosumtwi Crater Rocks

	Run 1		Run 2		Run 3		Run 4		Run 5		Run 6	
	Calc.	$\Delta_{obs-calc}$	Calc.	$\Delta_{obs-calc}$	Calc.	$\Delta_{obs-calc}$	Calc.	$\Delta_{obs-calc}$	Calc.	$\Delta_{obs-calc}$	Calc.	$\Delta_{obs-calc}$
SiO_2	67.15	0.43	66.98	0.60	67.14	0.44	67.16	0.42	67.15	0.43	67.14	0.44
TiO_2	0.57	-0.01	0.57	-0.01	0.57	-0.01	0.57	-0.01	0.57	-0.01	0.57	-0.01
Al_2O_3	16.58	0.16	16.50	0.24	16.55	0.19	16.55	0.19	16.54	0.20	16.54	0.20
Fe_2O_3	6.79	-0.01	6.72	0.06	6.74	0.04	6.73	0.05	6.73	0.05	6.73	0.05
MgO	3.46	0.0	3.39	0.07	3.24	0.22	3.18	0.28	3.20	0.26	3.20	0.26
CaO	1.33	0.05	1.36	0.02	-	-	-	-	-	-	-	-
K_2O	1.93	0.02	-	-	-	-	-	-	-	-	-	-
Sc	-	-	-	-	-	-	15.3	-0.6	15.3	-0.6	15.3	-0.6
Rb	-	-	-	-	-	-	64.4	1.6	64.3	1.7	64.3	1.7
Zr	-	-	-	-	-	-	130	4	130	4	130	4
La	-	-	-	-	-	-	-	-	-	-	20.6	0.1
Yb	-	-	-	-	-	-	-	-	-	-	1.81	-0.02
Hf	-	-	-	-	-	-	-	-	3.46	-0.08	3.46	-0.08
Th	-	-	-	-	-	-	-	-	3.44	0.10	3.44	0.10

All data in wt%. $\Delta_{obs-calc}$ = observed value (Table 2b) minus calculated value.

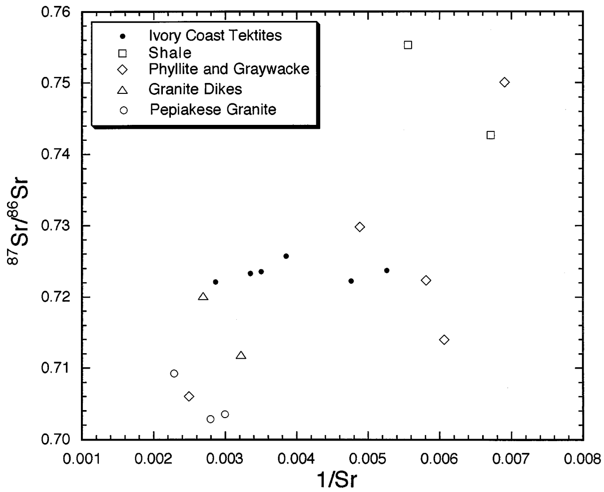

Fig. 10. $^{87}Sr/^{86}Sr$ vs. 1/Sr (ppm) for Ivory Coast tektites and Bosumtwi crater target rocks from this study and Shaw and Wasserburg (1982).

century, and its origin (volcanic, subsidence, or impact) was the subject of discussions for most of this century. The crater is located within a region containing about 2.1–2.2 Ma old metasediments and metavolcanics of the Birimian Supergroup. In the 1960s, several discoveries supporting an impact origin were made, including the presence of high-pressure quartz polymorphs, shocked minerals, and high-temperature minerals in melt fragments from suevitic breccia, and the presence of a possible meteoritic component in crater glasses. Furthermore, the crater, which is 1.07 Ma old, has been suggested as a likely source of the Ivory Coast tektites that are found on land at Cote d'Ivoire and in deep sea sediments in the Western Atlantic. As no integrated petrographical and geochemical studies of rocks from the Bosumtwi impact crater are available, this study attempts to fill this gap.

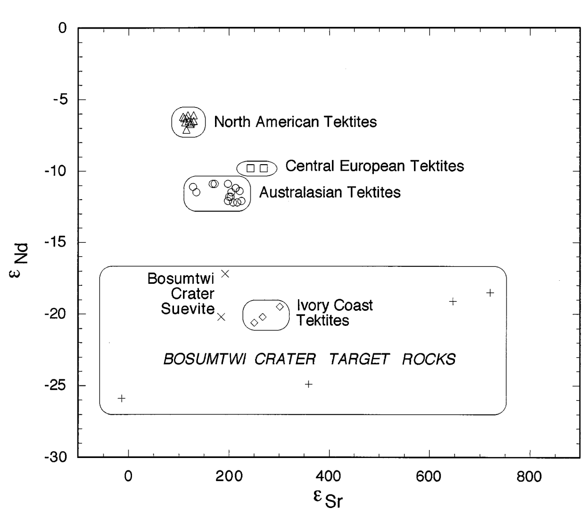

Fig. 11. ϵ_{Nd} vs. ϵ_{Sr} for tektites from all four strewn fields, as well as suevitic melt fragments and target rocks from the Bosumtwi crater. Tektite data from this study, Shaw and Wasserburg (1982), and Blum et al. (1992).

Our main observations and conclusions are summarized in the following paragraphs.

(1) We studied the petrographic and geochemical characteristics of twenty-three rocks from the Bosumtwi impact crater, which are thought to represent the range of target rocks present at the structure. The rocks, which are from the collections of Jones (1985a) and the Smithsonian Institution, can be classified into four groups: shale, phyllite-graywacke, granites found at small dikes that are dispersed in the crater area ("granite dikes"), and granitoids from a larger intrusive body near Pepiakese at the northeastern section of the crater ("Pepiakese granite"). For comparison, we also studied some melt fragments derived from suevitic breccia.
(2) Most of the studied samples are more or less strongly altered metasedimentary rocks, including phyllite, graywacke, and shale. None of the target rocks show any unambiguous evidence of shock metamorphism (i.e., planar deformation features, PDFs), but several of them show significant fracturing. Distinct impact-characteristic shock effects (PDFs) were identified only in clasts within suevite-derived melt fragments.
(3) The chemical compositions of the target rocks show considerable variations, with the largest differences between individual samples being displayed by the Pepiakese granite samples, and the least variation being shown by the metasedimentary rocks. The same is also true for the O and Sr isotopic composition of these rocks. The Pepiakese granites show petrographical and geochemical evidence of significant alteration.
(4) In a Rb-Sr isotope evolution diagram, the samples plot close to a best-fit line that yields an "age" of 1.98 Ga, with an initial $^{87}Sr/^{86}Sr$ ratio of 0.701, which is close to results previously obtained for granitoid intrusions in the Birimian of Ghana. Our measured Nd isotopic characteristics, with depleted mantle model ages ranging from 2.16 to 2.64 Ga, and ϵ_{Nd} values of -17.2 to -25.9, are also similar to those of Birimian rocks from other parts of Ghana.
(5) In contrast to the large range in composition of the Bosumtwi crater target rocks, Ivory Coast tektites are very homogeneous in major and trace element composition. The REE patterns of the tektites do not show any distinct Eu anomaly, and the high absolute REE abundances and steep patterns (La_N/Yb_N ratios of about 8), in agreement with the values observed for the metasedimentary rocks from the Bosumtwi impact structure.
(6) Harmonic least-squares (HMX) mixing calculations were carried out to reproduce the composition of Ivory Coast tektites from a mixture of Bosumtwi crater rocks. The best results were obtained if selected major (Si, Ti, Al, Fe, Mg) and lithophile trace elements (Sc, Rb, Zr, La, Yb, Hf, Th) were used in the calculations, yielding mixtures of about 70% phyllite-graywacke, 16% granite dike, and 14% Pepiakese granite. Shale does not occur as an important component (<2.5%).
(7) The oxygen isotopic composition of the metasedimentary rocks and granite dike ($\delta^{18}O$ = 11.3–13.6‰) and the tektites ($\delta^{18}O$ = 11.7–12.9‰, also this work) agree fairly well, while the Pepiakese granites have lower values

($\delta^{18}O = 8.6–9.0‰$), indicating that these rocks were not a major component in the formation of the Ivory Coast tektites. Furthermore, we determined the Sr and Nd isotopic characteristics of a selected number of Bosumtwi target rocks and Ivory Coast tektites, for comparison. The large variation in target rock compositions do not allow the unambiguous determination of distinct endmember compositions, but in both a $^{87}Sr/^{86}Sr$ vs. 1/Sr plot and an ϵ_{Sr} vs. ϵ_{Nd} diagram, the tektites plot within the field defined by the metasedimentary and granitic Bosumtwi crater rocks.

(8) Despite the spread in rock type and chemical and isotopic composition of the presently available, somewhat limited set of Bosumtwi crater rocks, our data support the conclusion that the Ivory Coast tektites were formed from the same rocks that are currently exposed at the Bosumtwi crater, and during the same impact event that formed the Bosumtwi crater. The suevitic glasses show a much wider range in composition than the tektites and have preserved the variety of country rocks in much more detail than the homogenized tektites.

Acknowledgements—The research was supported by the Austrian "Fonds zur Förderung der wissenschaftlichen Forschung," Projects P09021-GEO and START Y-58 (to CK), and NSF PFF grant EAR9350262 (to JDB). We thank Willy B. Jones (Wrexham, UK) for making rock samples from his original study available, the Smithsonian Institution (Washington, DC, USA) for additional rock samples, Dona Jalufka (Vienna) for preparing some of the line drawings, and Cynthia Blum (Hanover, New Hampshire, USA) for help with isotope analyses. We are grateful to R. Anderson and an anonymous reviewer for helpful reviews of the manuscript.

REFERENCES

Bampo S. O. (1963) Kumasi conference on the Lake Bosumtwi crater. *Nature* **198,** 1150–1151.

Blum J. D. (1995) Isotope decay data. In *Handbook of Physical Constants* (ed. T. J. Ahrens), pp. 271–282. AGU.

Blum J. D. and Chamberlain C. P. (1992) Oxygen isotope constraints on the origin of impact glasses from the Cretaceous-Tertiary boundary. *Science* **257,** 1104–1107.

Blum J. D., Papanastassiou D. A., Koeberl C., and Wasserburg, G. J. (1992) Neodymium and strontium isotopic study of Australasian tektites: New constraints on the provenance and age of target materials. *Geochim. Cosmochim. Acta* **56,** 483–492.

Blum J. D., Chamberlain C. P., Hingston M. P., and Koeberl C. (1996) Neodymium, strontium, and oxygen isotope investigation of the target stratigraphy and impact melt rocks from the Manson impact structure, Iowa, USA. In *The Manson Impact Structure, Iowa: Anatomy of an Impact Crater* (ed. C. Koeberl and R. R. Anderson); GSA Special Paper **302,** 317–324.

Bollinger K. (1993) ^{40}Ar-^{39}Ar Datierung von Tektiten. Diplomarbeit, Max-Planck-Institut, Heidelberg, and Ruprecht-Karls-Universität Heidelberg.

Cande S. C. and Kent D. V. (1995) Revised calibration of the geomagnetic timescale for the Late Cretaceous and Cenozoic. *J. Geophys. Res.* **100,** 6093–6095.

Chamberlain C. P., Blum J. D., and Koeberl C. (1993) Oxygen isotopes as tracers of tektite source rocks: An example from the Ivory Coast tektites and Lake Bosumtwi crater. *Lunar Planet. Sci.* **XXIV,** 267–268.

Chao E. C. T. (1968) Pressure and temperature histories of impact metamorphosed rocks—based on petrographic observations. In *Shock Metamorphism of Natural Materials* (ed. B. M. French and N. M. Short), pp. 135–158. Mono Book Corp.

Chapman D. R., and Scheiber L. C. (1969) Chemical investigation of Australasian tektites. *J. Geophys. Res.* **74,** 6737–6776.

Chaussidon M. and Koeberl C. (1995) Boron content and isotopic composition of tektites and impact glasses: Constraints on source regions. *Geochim. Cosmochim. Acta* **59,** 613–624.

Clayton R. N. and Mayeda T. K. (1963) The use of bromine pentaflouride in the extraction of oxygen from oxides and silicates for isotope analysis. *Geochim. Cosmochim. Acta* **27,** 43-52.

Cuttitta F., Carron M. K., and Annell C. S. (1972) New data on selected Ivory Coast tektites. *Geochim. Cosmochim. Acta* **36,** 1297–1309.

Davis D. W., Hirdes W., Schaltegger U., and Nunoo E. A. (1994) U-Pb age constraints on deposition and provenance of Birimian and gold-bearing Tarkwaian sediments in Ghana, West Africa. *Precambr. Res.* **67,** 89–107.

DePaolo D. J. (1981) Neodymium isotopes in the Colorado front range and crust-mantle evolution in the Proterozoic. *Nature* **291,** 193–196.

Durrani J. A. and Khan H. A. (1971) Ivory Coast microtektites: Fission track ages and geomagnetic reversals. *Nature* **323,** 320–323.

El Goresy A. (1966) Metallic spherules in Bosumtwi crater glasses. *Earth Planet. Sci. Lett.* **1,** 23–24.

El Goresy A., Fechtig H., and Ottemann T. (1968) The opaque minerals in impactite glasses. In *Shock Metamorphism of Natural Materials* (ed. B. M. French and N. M. Short), pp. 531–554. Mono Book Corp.

Engelhardt W. v., Luft E., Arndt J., Schock H., and Weiskirchner W. (1987) Origin of moldavites. *Geochim. Cosmochim. Acta* **51,** 1425–1443.

Fergusson M. (1902) Lake Bosumchwi. *Geogr. J.* **19,** 370–372.

Fleischer R. L., Price P. B., and Walker R. M. (1965) On the simultaneous origin of tektites and other natural glasses. *Geochim. Cosmochim. Acta* **29,** 161–166.

Gentner W. (1966) Auf der Suche nach Kratergläsern, Tektiten und Meteoriten in Afrika. *Naturwissenschaften* **12,** 285–289.

Gentner W., Lippolt H. J., and Müller O. (1964) Das Kalium-Argon-Alter des Bosumtwi Kraters in Ghana und die chemische Beschaffenheit seiner Gläser. *Z. Naturforsch.* **19A,** 150–153.

Gentner W., Kleinmann B., and Wagner G. A. (1967) New K-Ar and fission track ages of impact glasses and tektites. *Earth Planet. Sci. Lett.* **2,** 83–86.

Gentner W., Storzer D., and Wagner G. A. (1969a) Das Alter von Tektiten und verwandten Gläsern. *Naturwissenschaften* **56,** 255–261.

Gentner W., Storzer D., and Wagner G. A. (1969b) New fission track ages of tektites and related glasses. *Geochim. Cosmochim. Acta* **33,** 1075–1081.

Glass B. P. (1968) Glassy objects (microtektites?) from deep sea sediments near the Ivory Coast. *Science* **161,** 891–893.

Glass B. P. (1969) Chemical composition of Ivory Coast microtektites. *Geochim. Cosmochim. Acta* **33,** 1135–1147.

Glass, B. P. and Pizzuto, J. E. (1994) Geographic variations in Australasian microtektite concentrations: Implications concerning the location and size of the source crater. *J. Geophys. Res.* **99,** 19075–19081.

Glass B. P. and Zwart P. A. (1979) The Ivory Coast microtektite strewn field: New data. *Earth Planet. Sci. Lett.* **43,** 336–342.

Glass B. P., Swincki M. B., and Zwart P. A. (1979) Australasian, Ivory Coast and North American tektite strewn field: Size, mass and correlation with geomagnetic reversals and other earth events. *Proc. 10th Lunar Planet. Sci. Conf.* 2535–2545.

Glass B. P., Kent D. V., Schneider D. A., and Tauxe L. (1991) Ivory Coast microtektite strewn field: Description and relation to the Jaramillo geomagnetic event. *Earth Planet. Sci. Lett.* **107,** 182–196.

Glass B. P., Koeberl C., Senftle F., Blum J. D., Izett G. A., Povenmire H., and Strange R. L. (1995) A Muong Nong type Georgia tektite. *Geochim. Cosmochim. Acta* **59,** 4071–4082.

Grieve R. A. F., Langenhorst F., and Stöffler D. (1996) Shock metamorphism of quartz in nature and experiment: II. Significance in geoscience. *Meteoritics Planet. Sci.* **31,** 6–35.

Hirdes W., Davis D. W., and Eisenlohr B. N. (1992) Reassessment of Proterozoic granitoid ages in Ghana on the basis of U/Pb zircon and monazite dating. *Precambr. Res.* **56,** 89–96.

Hirdes W., Davis D. W., Lüdtke G., and Konan G. (1996) Two generations of Birimian (Paleoproterozoic) volcanic belts in north-eastern Cǒte d'Ivoire (West Africa): Consequences for the "Birimian controversy." *Precambr. Res.* **80,** 173–191.

Jones W. B. (1983) A proposed gas pool in the Pleistocene Bosumtwi impact crater, Ghana. *J. Petrol. Geol.* **5,** 315–318.

Jones W. B. (1985a) Chemical analyses of Bosumtwi crater target rocks compared with Ivory Coast tektites. *Geochim. Cosmochim. Acta* **49,** 2569–2576.

Jones W. B. (1985b) The origin of the Bosumtwi crater, Ghana—an historical review. *Proc. Geol. Assoc. London* **96,** 275–284.

Jones W. B., Bacon M., and Hastings D. A. (1981) The Lake Bosumtwi impact crater, Ghana. *GSA Bull.* **92,** 342–349.

Junner N. R. (1937) The geology of the Bosumtwi caldera and surrounding country. *Gold Coast Geol. Surv. Bull.* **8,** 1–38.

Kitson A. K. (1916) The Gold Coast: Some consideration of its structure, people and natural history. *Geogr. J.* **48,** 369–392.

Koeberl C. (1993) Instrumental neutron activation analysis of geochemical and cosmochemical samples: A fast and proven method for small sample analysis. *J. Radioanalyt. Nuclear Chem.* **168,** 47–60.

Koeberl C. (1994) Tektite origin by hypervelocity asteroidal or cometary impact: Target rocks, source craters, and mechanisms. In *Large Meteorite Impacts and Planetary Evolution* (ed. B. O. Dressler et al.); *GSA Special Paper* **293,** 133–151.

Koeberl C. and Reimold W. U. (1996) Lake Bosumtwi, Ghana, impact structure: Petrography and geochemistry of target rocks. *Meteoritics Planet. Sci.* **31,** A72.

Koeberl C. and Shirey S. B. (1993) Detection of a meteoritic component in Ivory Coast tektites with rhenium-osmium isotopes. *Science* **261,** 595–598.

Koeberl C., Kluger F., and Kiesl W. (1987) Rare earth element determinations at ultratrace abundance levels in geologic materials. *J. Radioanalyt. Nuclear Chem.* **112,** 481–487.

Koeberl C., Bottomley R. J., Glass B. P., and Storzer D. (1997a) Geochemistry and age of Ivory Coast tektites and microtektites. *Geochim. Cosmochim. Acta* **61,** 1745–1772.

Koeberl C., Reimold W. U., Pesonen L. J., and Brandt D. (1997b) New Studies of the Bosumtwi Impact Structure, Ghana: The 1997 Field Season. *Meteoritics Planet. Sci.* **32,** A72–A73.

Kolbe P., Pinson W. H., Saul J. M., and Miller E. W. (1967) Rb-Sr study on country rocks of the Bosumtwi crater, Ghana. *Geochim. Cosmochim. Acta* **31,** 869–875.

Lacroix A. (1934) Sur la découverte de tectites à la Cŏte d'Ivoire. *C. R. Acad. Sci. Paris* **199,** 1539–1542.

Leube A., Hirdes W., Mauer R., and Kesse G. O. (1990) The early Proterozoic Birimian Supergroup of Ghana and some aspects of its associated gold mineralization. *Precambr. Res.* **46,** 139–165.

Lippolt H. J. and Wasserburg G. J. (1966) Rubidium-Strontium-Messungen an Gläsern vom Bosumtwi-Krater und an Elfenbeinküsten-Tektiten. *Z. Naturforsch.* **21A,** 226–231.

Littler J., Fahey J. J., Dietz R. S., and Chao E. C. T. (1961) Coesite from the Lake Bosumtwi crater, Ashanti, Ghana. *GSA Special Paper* **68,** 218.

Maclaren M. (1931) Lake Bosumtwi, Ashanti. *Geogr. J.* **78,** 270–276.

Moon P. A. and Mason D. (1967) The geology of 1/4 field sheets nos. 129 and 131, Bompata S.W. and N.W. *Ghana Geol. Surv. Bull.* **31,** 1–51.

Palme H., Janssens M.-J., Takahasi H., Anders E., and Hertogen J. (1978) Meteorite material at five large impact craters. *Geochim. Cosmochim. Acta* **42,** 313–323.

Palme H., Grieve R. A. F., and Wolf R. (1981) Identification of the projectile at the Brent crater, and further considerations of projectile types at terrestrial craters. *Geochim. Cosmochim. Acta* **45,** 2417–2424.

Pinson W. H., and Griswold T. B. (1969) The relationship of nickel and chromium in tektites: New data on the Ivory Coast tektites. *J. Geophys. Res.* **74,** 6811–6815.

Reimold W. U., Koeberl C., and Bishop J. (1994) Roter Kamm impact crater, Namibia: Geochemistry of basement rocks and breccias. *Geochim. Cosmochim. Acta* **58,** 2689–2710.

Reimold W. U., Brandt D., and Koeberl C. (1997) Geological studies at Lake Bosumtwi impact crater, Ghana. *Meteoritics Planet. Sci.* **32,** A107.

Reimold W. U., Brandt D., and Koeberl C. (1998) Detailed structural analysis of the rim of a large, complex impact crater: Bosumtwi crater, Ghana. *Geology* **26,** 543–546.

Rohleder H. P. T. (1936) Lake Bosumtwi, Ashanti. *Geogr. J.* **87,** 51–65.

Rybach L. and Adams J. A. S. (1969) The radioactivity of the Ivory Coast tektites and the formation of the Bosumtwi crater (Ghana). *Geochim. Cosmochim. Acta* **33,** 1101–1102.

Saul J. M. (1969) *Field investigations at Lake Bosumtwi (Ghana) and in the Ivory Coast tektite strewn field.* National Geographic Society Research Reports, 1964 Proj., 201–212.

Schneider D. A. and Kent D. V. (1990) Ivory Coast microtektites and geomagnetic reversals. *Geophys. Res. Lett.* **17,** 163–166.

Schnetzler C. C., Pinson W. H., and Hurley P. M. (1966) Rubidium-Strontium age of the Bosumtwi crater area, Ghana, compared with the age of the Ivory Coast tektites. *Science* **151,** 817–819.

Schnetzler C. C., Philpotts J. A., and Thomas H. H. (1967) Rare earth and barium abundances in Ivory Coast tektites and rocks from the Bosumtwi crater area, Ghana. *Geochim. Cosmochim. Acta* **31,** 1987–1993.

Shaw H. F. and Wasserburg G. J. (1982) Age and provenance of the target materials for tektites and possible impactites as inferred from Sm-Nd and Rb-Sr systematics. *Earth Planet. Sci. Lett.* **60,** 155–177.

Smit A. F. J. (1964) Origin of Lake Bosumtwi, Ghana. *Nature* **131,** 117–118.

Stöckelmann D. and Reimold W. U. (1989) The HMX mixing calculation program. *Math. Geol.* **21,** 853–860.

Storzer D. and Wagner G. A. (1977) Fission track dating of meteorite impacts. *Meteoritics* **12,** 368–369.

Taylor H. P. and Epstein S. (1966) Oxygen isotope studies of Ivory Coast tektites and impactite glass from the Bosumtwi crater, Ghana. *Science* **153,** 173–175.

Taylor H. P. and Epstein S. (1969) Correlations between O^{18}/O^{16} ratios and chemical compositions of tektites. *J. Geophys. Res.* **74,** 6834–6844.

Taylor H. P. and Sheppard S. M. F. (1986) Igneous Rocks: I. Processes of isotopic fractionation and isotope systematics. In *Stable isotopes in high temperature geological processes* (ed. J. W. Valley et al.); *Rev. Mineral.* **16** 227-272. MSA.

Taylor P. N., Moorbath S., Leube A., and Hirdes W. (1992) Early Proterozoic crustal evolution in the Birimian of Ghana: Constraints from geochronology and isotope geochemistry. *Precambr. Res.* **56,** 97–111.

Taylor S. R. and McLennan S. M. (1985) *The Continental Crust: Its Composition and Evolution.* Blackwell.

Tera F., Middleton R., Klein J., and Brown L. (1983a) Beryllium-10 in tektites. *EOS Trans. AGU* **64,** 284.

Tera F., Brown L., Klein J., and Middleton R. (1983b) Beryllium-10: Tektites. *Yearb. Carnegie Inst. 1982,* 463–465.

Turner B. F., Gardner L. R., and Sharp W.E. (1996) The hydrology of Lake Bosumtwi, a climate-sensitive lake in Ghana, West Africa. *J. Hydrol.* **183,** 243–261.

Woodfield P.D. (1966) The geology of the 1/4 field sheet 91, Fumso, N.W. *Ghana Geol. Surv. Bull.* 30.

Wright J. B., Hastings D. A., Jones W. B., and Williams H. R. (1985) Geology and Mineral Resources of West Africa. Allen and Unwin.

York D. (1969) Least squares fitting of a straight line with correlated errors. *Earth. Planet. Sci. Lett.* **5,** 320–324.

Zähringer J. (1963) K-Ar measurements of tektites. In *Radioactive Dating,* pp. 289–305. IAEA.